PromptRestorer: A Prompting Image Restoration Method with Degradation Perception —Supplementary Materials—

Cong Wang[1]*, **Jinshan Pan**[2]*, **Wei Wang**[3]*, **Jiangxin Dong**[2], **Mengzhu Wang**[4], **Yakun Ju**[1], **Junyang Chen**[5]
[1]The Hong Kong Polytechnic University, [2]Nanjing University of Science and Technology,
[3]Dalian University of Technology, [4]Hebei University of Technology, [5]Shenzhen University

Abstract

In this supplementary material, we first describe the datasets used in various restoration tasks and experimental details in Sec. 1. Then, we demonstrate the superiority of the proposed PromptDMP compared with commonly used feature fusion module-Spatial Feature Transform (SFT) [27] in Sec. 2. And then, we validate the effectiveness of the used improved ConvNeXt compared with ConvNeXt [21] in Sec. 3. Next, we present the detailed structure of the pre-trained encoder in Sec. 4. Last, we provide additional visual results compared to state-of-the-art approaches on various image restoration tasks in Sec. 5.

1 Datasets Description and Experimental Details

For different restoration tasks, the training and testing datasets are described in Tab. 1.

Image Deraining: In accordance with [15, 31, 8], we utilize a composite training dataset consisting of 13,712 image pairs collected from various training datasets, namely Rain100H [30], Rain100L [30], Test100 [34], Test1200 [33], and Test2800 [10]. PromptRestorer is evaluated on Rain100H [30], Rain100L [30], Test100 [34], Test1200 [33], and Test2800 [10]. Our PromptRestorer model is trained for 600 epochs.

Image Deblurring: Consistent with recent methods [29, 31], we train PromptRestorer using the GoPro dataset [22]. The GoPro dataset comprises 2,103 blurry/sharp image pairs for training and 1,111 pairs for evaluation. To assess the generalization capacity of our method, we directly apply the GoPro-trained model to the HIDE dataset [24] and the real-world benchmark RSBlur [23]. Our network is trained for 3,000 epochs on the GoPro dataset.

Image Dehazing: For dehazing, we train PromptRestorer on the commonly used RESIDE dataset [16]. We employ the ITS dataset for training and use SOTS-indoor as the testing dataset. PromptRestorer is trained for 600 epochs on ITS. Additionally, following [12], we include the real-world datasets Dense-Haze [1] and NH-Haze [2] as experimental datasets, containing 45 training images and 5 testing images, respectively. The network is trained on Dense-Haze and NH-Haze for 3,000 epochs.

Image Desnowing: For desnowing, we utilize the CSD [6], SRRS [5], and Snow100K [20] datasets. Following previous works [4], we randomly sample 2,500 image pairs from the training set for training and 2,000 images from the testing set for evaluation. The model is trained for 1,000 epochs on each dataset.

*These authors equally contribute to this work.

37th Conference on Neural Information Processing Systems (NeurIPS 2023).

Table 1: **Dataset description** for various image restoration tasks.

Tasks	**Datasets**	**Train Samples**	**Test Samples**	**Testset Rename**
Deraining	Rain14000 [10]	11200	2800	Test2800
	Rain1800 [30]	1800	0	-
	Rain800 [34]	700	100	Test100
	Rain100H [30]	0	100	Rain100H
	Rain100L [30]	0	100	Rain100L
	Rain1200 [33]	0	1200	Test1200
	Rain12 [18]	12	0	-
Deblurring	GoPro [22]	2103	1111	-
	HIDE [24]	0	2025	-
	RSBlur [23]	0	1960	-
Dehazing	RESIDE/ITS [16]	13990	500	SOTS-Indoor
	Dense-Haze [1]	45	5	-
	NH-Haze [2]	45	5	-
Desnowing	CSD [6]	2500	2000	CSD (2000)
	SRRS [5]	2500	2000	SRRS (2000)
	Snow100K [20]	2500	2000	Snow100K (2000)

2 PromptDMP vs. Spatial Feature Transform (SFT) [27]

Spatial Feature Transform (SFT) [27] which usually generates affine transformation parameters for spatial-wise feature modulation is a commonly used feature fusion module to bridge the feature transformation between conditional features and restoration features [28, 13, 11, 7]. Hence, one may wonder to know whether our proposed PromptDMP is more effective than SFT or not. To validate this, we replace our PromptDMP with SFT to conduct ablation experiments. Tab. 2 shows that our PromptDMP improves the restoration quality by 0.316 dB compared with the results by SFT. It clearly demonstrates that our PromptDMP is more effective than SFT thanks to the designs of global and local prompting perception.

Table 2: **PromptDMP vs. SFT.** Our PromptDMP is more effective than the commonly used SFT [27].

Experiment	PSNR	FLOPs (G)	Params (M)
w/ SFT [27]	30.699	108.14	10.36
w/ PromptDMP (***Ours***)	**31.015**	146.36	13.24

3 Improved ConvNeXt vs. ConvNeXt [21]

We in this paper employ the improved ConvNeXt by using two depth-wise convolutions with 3×3 kernel sizes instead of ConvNeXt [21] which uses a depth-wise convolution with 7×7 kernel sizes. To validate the effectiveness of improved ConvNeXt, we use the ConvNeXt [21] to replace our used improved ConvNeXt, and the results are reported in Tab. 3. It shows that our improved ConvNeXt is more effective. This also reveals that stacking small kernel convolutions can learn better representations than a large kernel convolution with the equivalent receptive field for image restoration.

Table 3: **Improved ConvNeXt vs. ConvNeXt.** Our improved ConvNeXt can help produce high-quality restoration results compared with ConvNeXt [27].

Experiment	PSNR	FLOPs (G)	Params (M)
w/ ConvNeXt [21]	30.354	144.28	12.97
w/ Improved ConvNeXt (***Ours***)	**31.015**	146.36	13.24

4 Network Architecture of Pre-trained Encoder

We further specify the architecture of the encoder in Tab. 4. Note that the learnable conditions have the same encoder architecture as our pre-trained encoder for fair comparisons. The training process of our pre-trained VQGAN method follows [3].

Table 4: **Encoder architecture.** The encoder mainly consists of convolution layers, residual blocks [14], and downsample operation. The encoder gradually encodes input images to spatially-reduced features.

Layer	Encoder1	Downsample	Encoder2	Downsample	Encoder3
Shape	$48 \times H \times W$	$48 \times \frac{H}{2} \times \frac{W}{2}$	$96 \times \frac{H}{2} \times \frac{W}{2}$	$96 \times \frac{H}{4} \times \frac{W}{4}$	$192 \times \frac{H}{4} \times \frac{W}{4}$
Blocks	1 Conv & 2 ResBlocks	-	1 Conv & 2 ResBlocks	-	1 Conv & 2 ResBlocks
Kernel sizes	3×3	-	3×3	-	3×3
Stride	1	-	1	-	1

5 Addtional Visual Results

We provide more visual results on various image restoration tasks in Fig. 1-Fig. 38.

Image Deraining Results: Fig. 1-Fig. 4.

Image Deblurring Results: Fig. 5-Fig. 7.

Image Dehazing Results: Fig. 8-Fig. 24.

Image Desnowing Results: Fig. 25-Fig. 38.

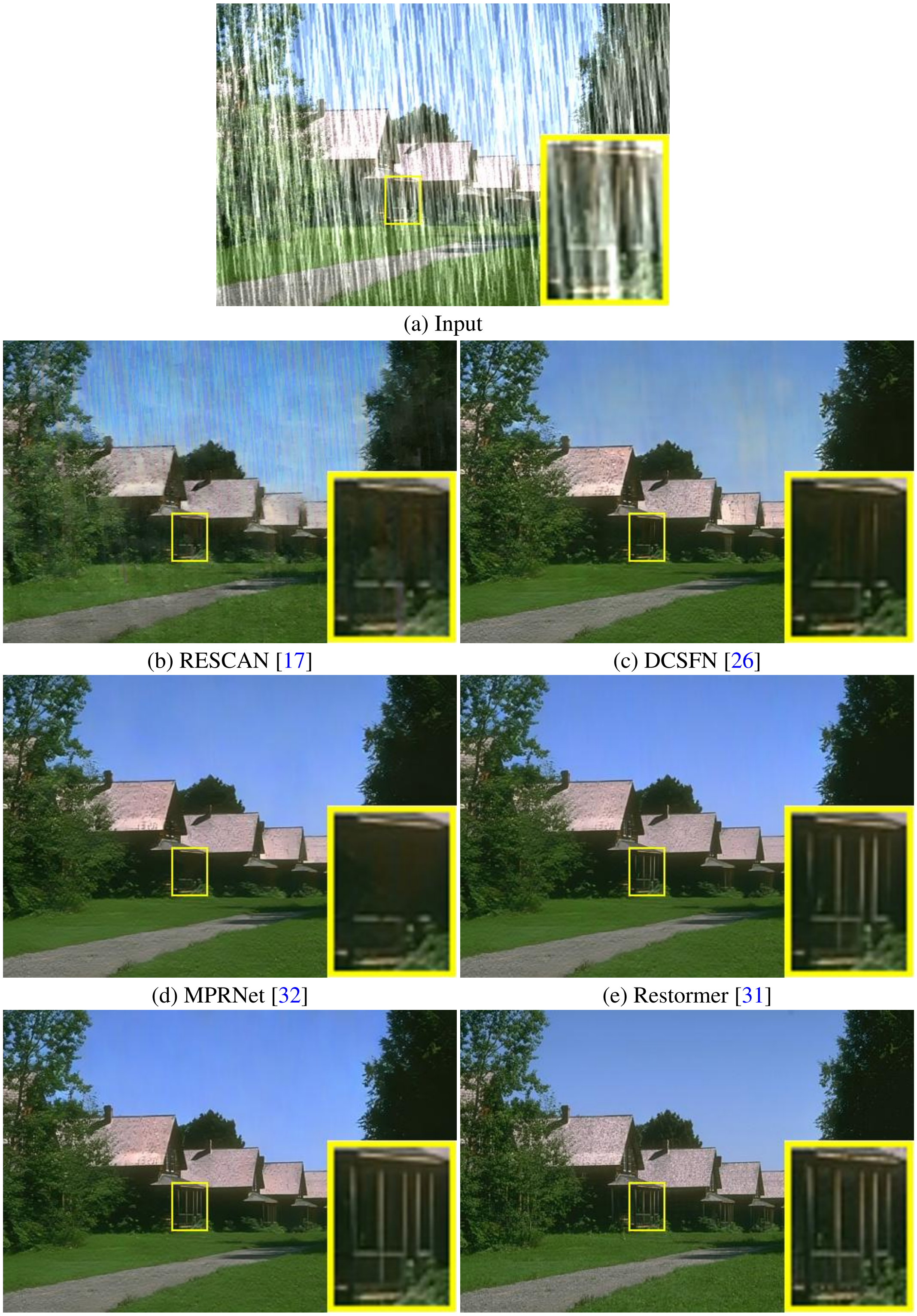

(a) Input

(b) RESCAN [17]

(c) DCSFN [26]

(d) MPRNet [32]

(e) Restormer [31]

(f) PromptRestorer

(g) GT

Figure 1: **Image deraining** example on Rain100H [30].

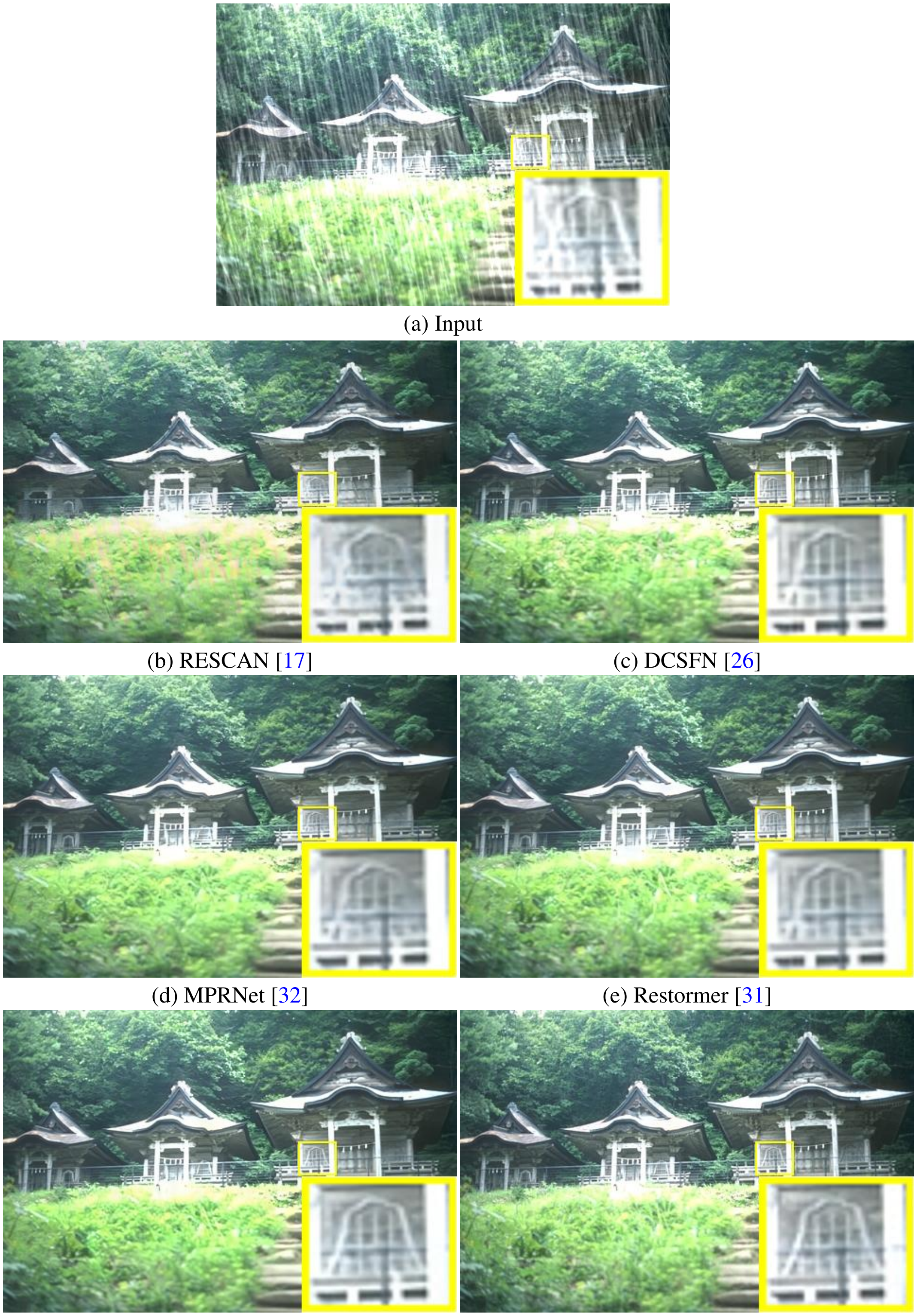

(a) Input

(b) RESCAN [17]

(c) DCSFN [26]

(d) MPRNet [32]

(e) Restormer [31]

(f) PromptRestorer

(g) GT

Figure 2: **Image deraining** example on Rain100H [30].

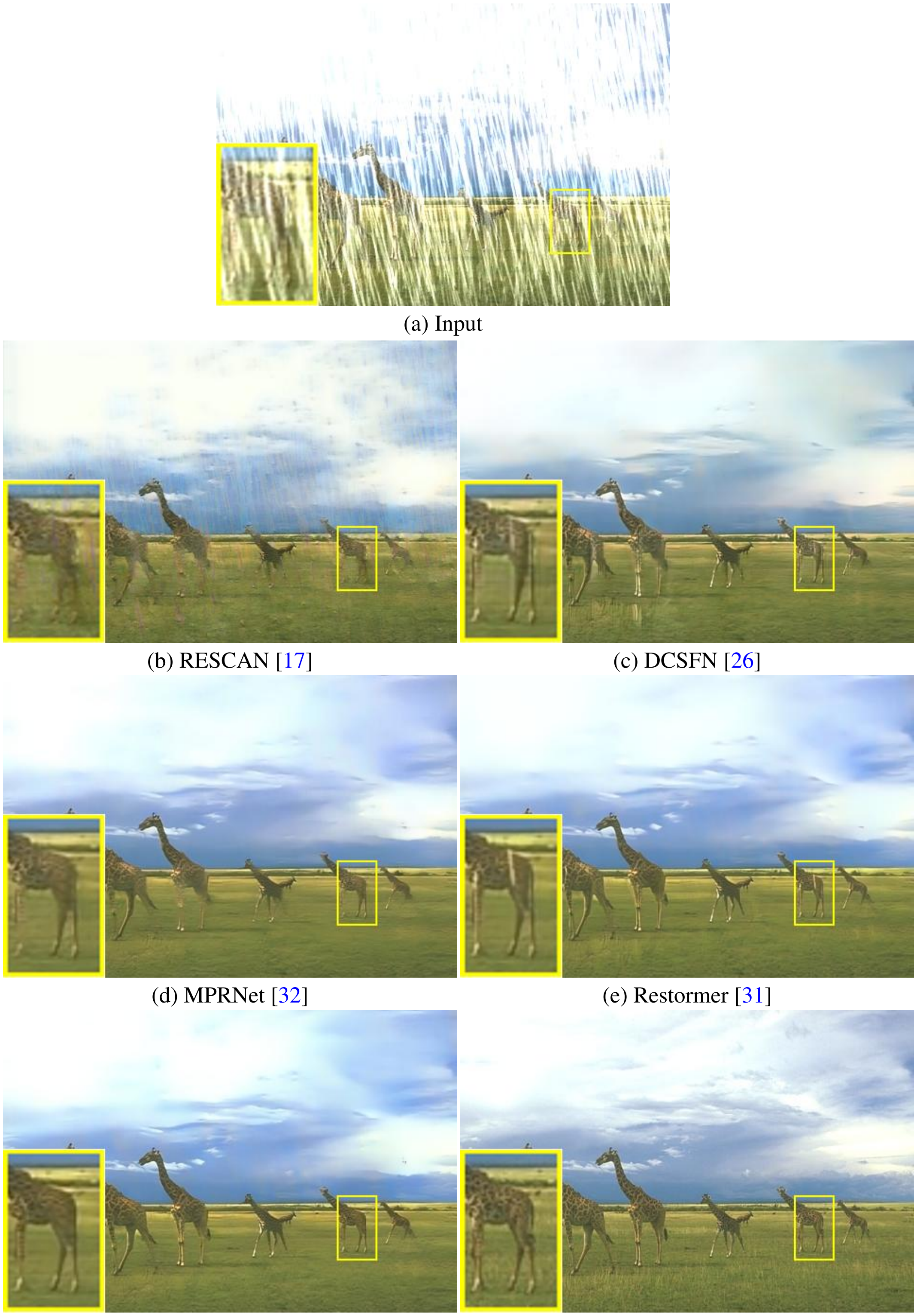

(a) Input

(b) RESCAN [17]

(c) DCSFN [26]

(d) MPRNet [32]

(e) Restormer [31]

(f) PromptRestorer

(g) GT

Figure 3: **Image deraining** example on Rain100H [30].

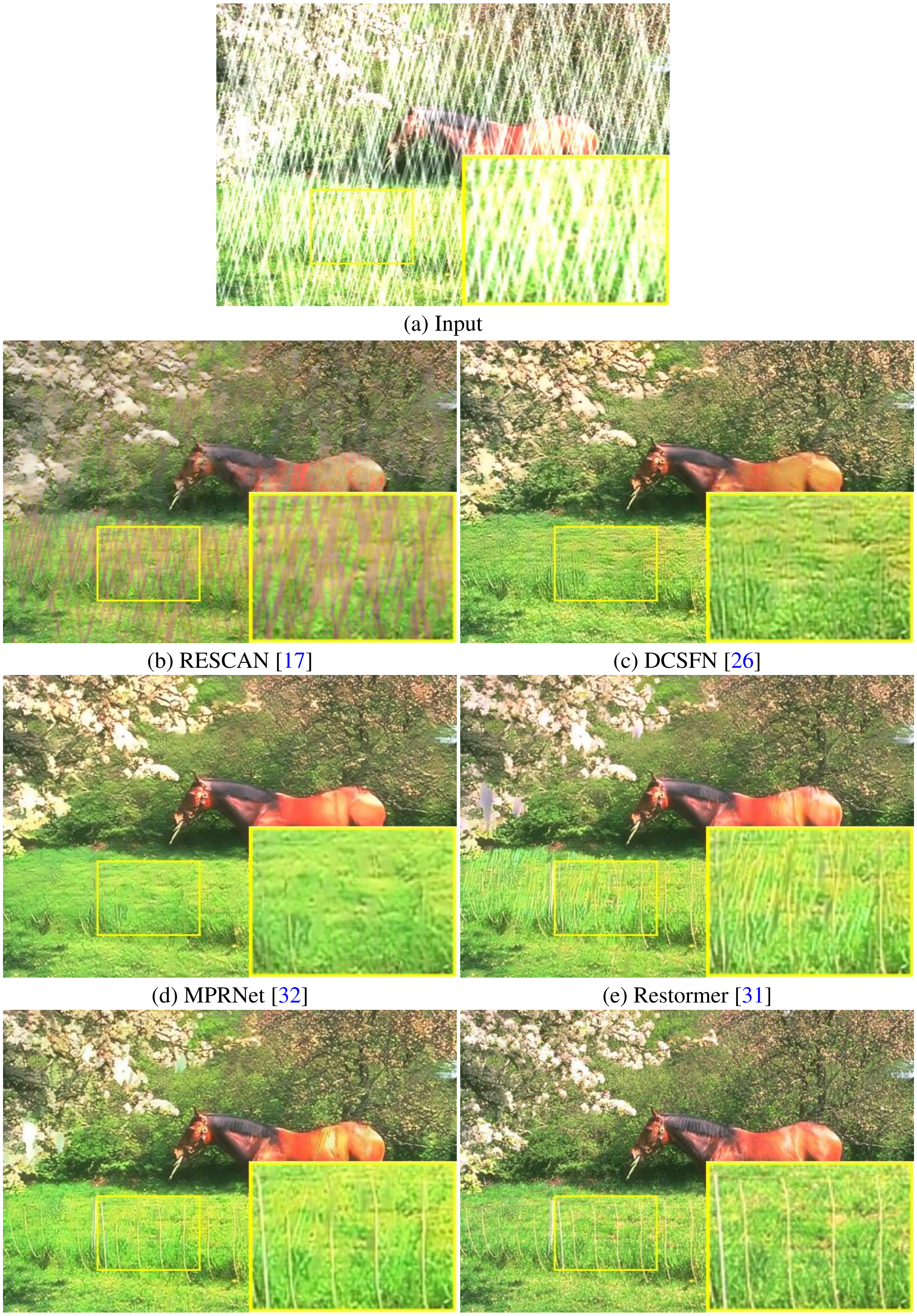

(a) Input

(b) RESCAN [17]

(c) DCSFN [26]

(d) MPRNet [32]

(e) Restormer [31]

(f) PromptRestorer

(g) GT

Figure 4: **Image deraining** example on Rain100H [30].

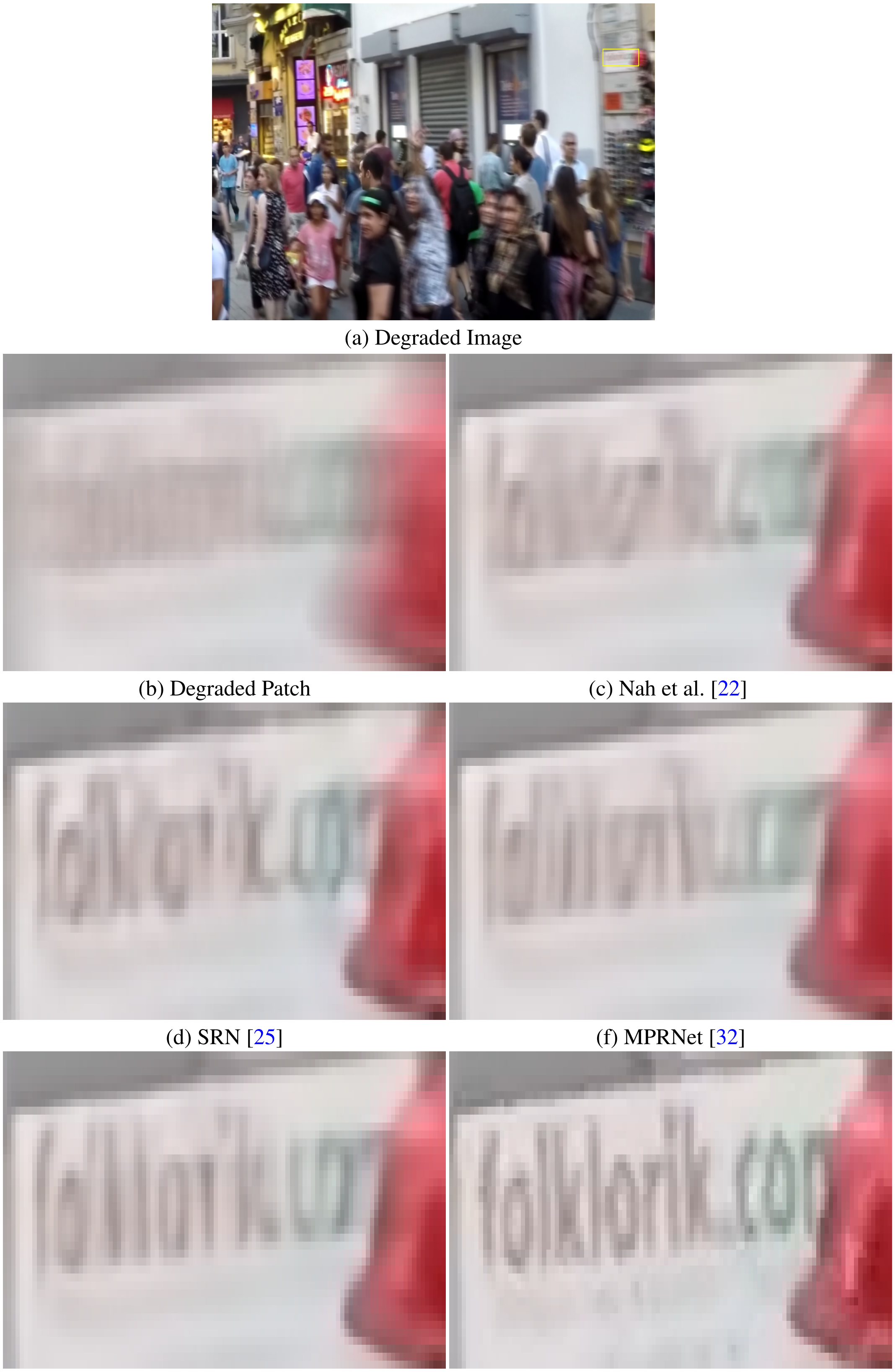

(a) Degraded Image

(b) Degraded Patch

(c) Nah et al. [22]

(d) SRN [25]

(f) MPRNet [32]

(g) PromptRestorer

(h) GT

Figure 5: **Image blurring** example on GoPro [22].

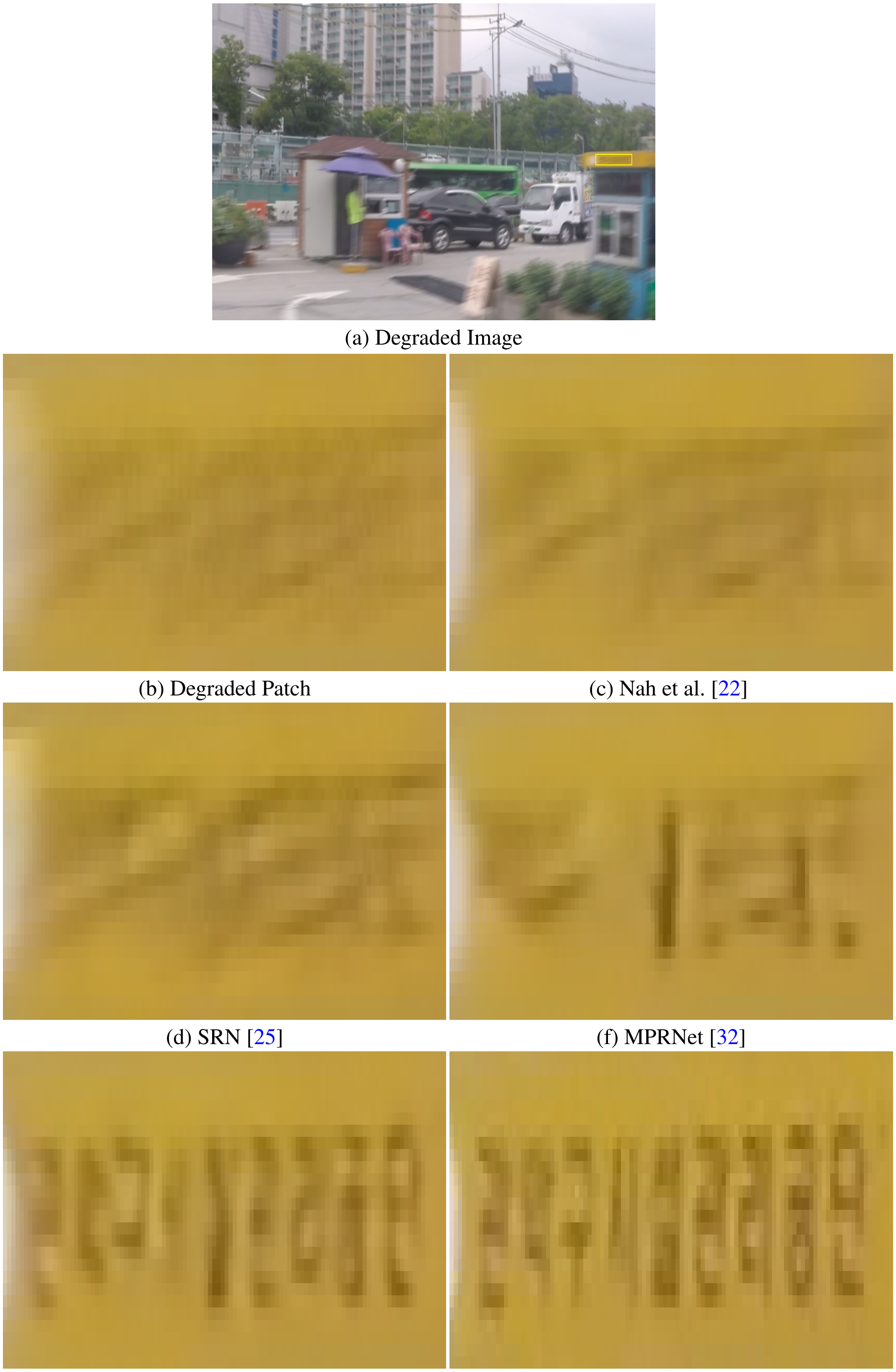

(a) Degraded Image

(b) Degraded Patch

(c) Nah et al. [22]

(d) SRN [25]

(f) MPRNet [32]

(g) PromptRestorer

(h) GT

Figure 6: **Image blurring** example on GoPro [22].

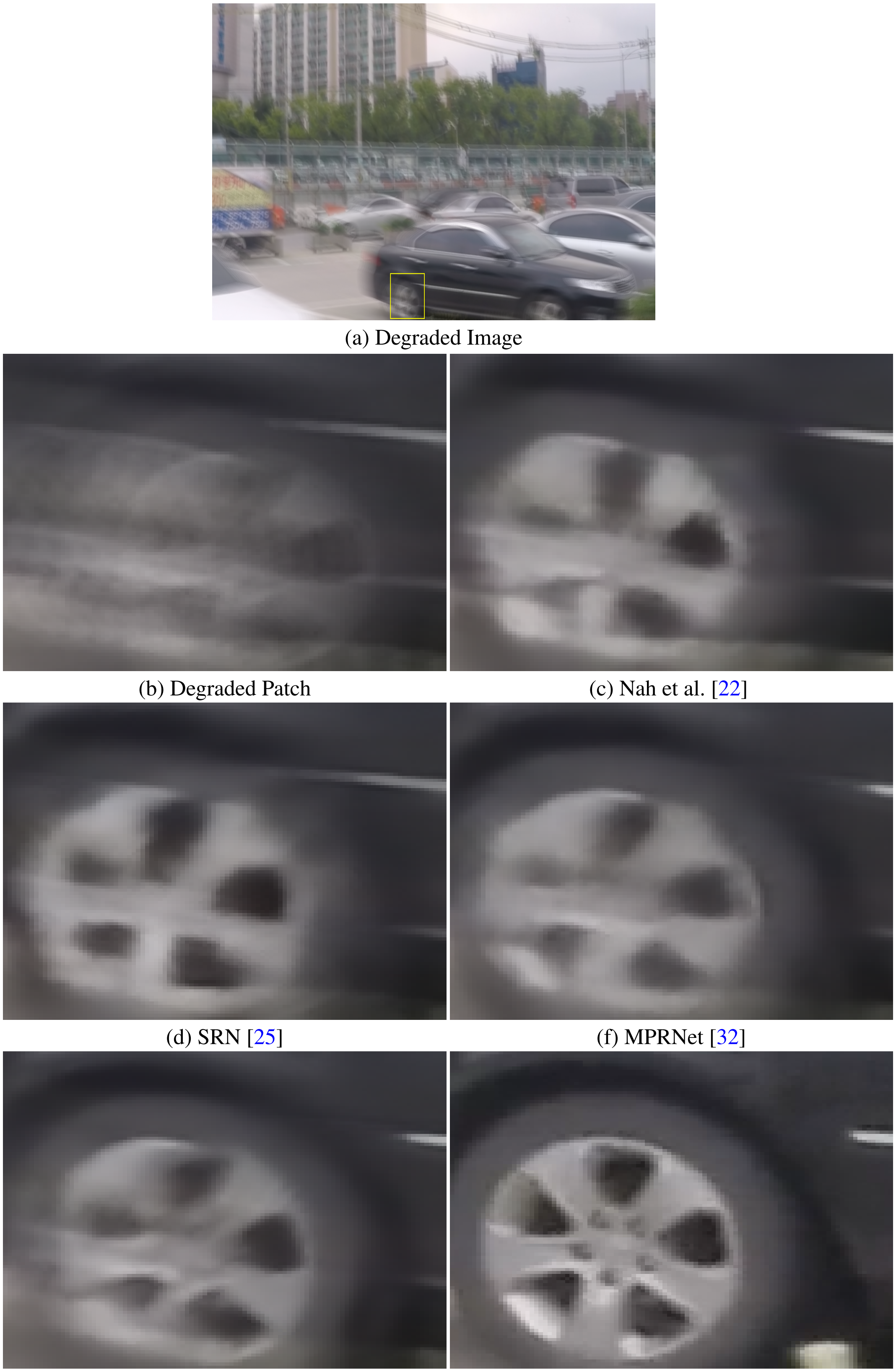

(a) Degraded Image

(b) Degraded Patch

(c) Nah et al. [22]

(d) SRN [25]

(f) MPRNet [32]

(g) PromptRestorer

(h) GT

Figure 7: **Image blurring** example on GoPro [22].

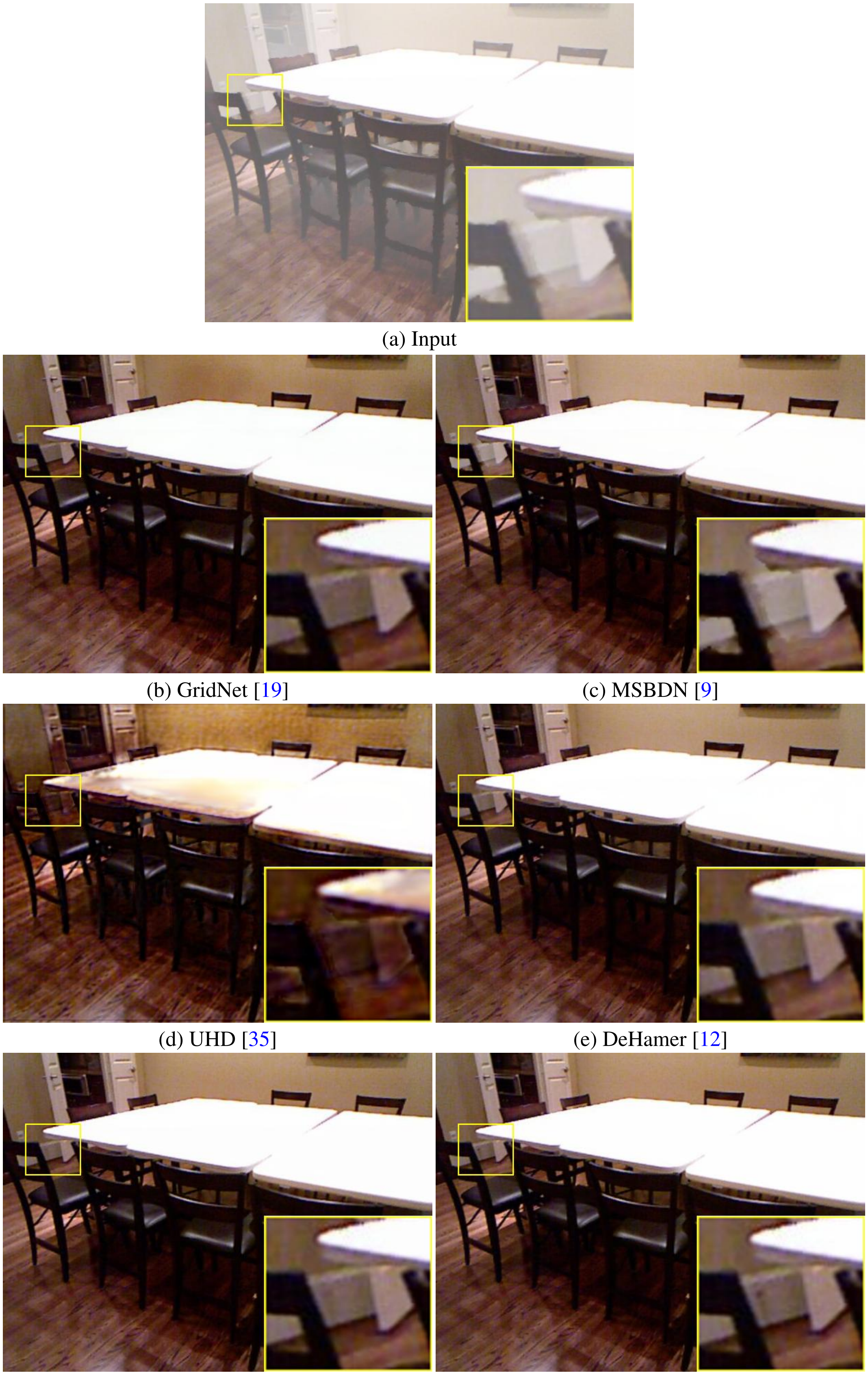

(a) Input

(b) GridNet [19]

(c) MSBDN [9]

(d) UHD [35]

(e) DeHamer [12]

(f) PromptRestorer

(g) GT

Figure 8: **Image dehazing** example on SOTS-Indoor [16].

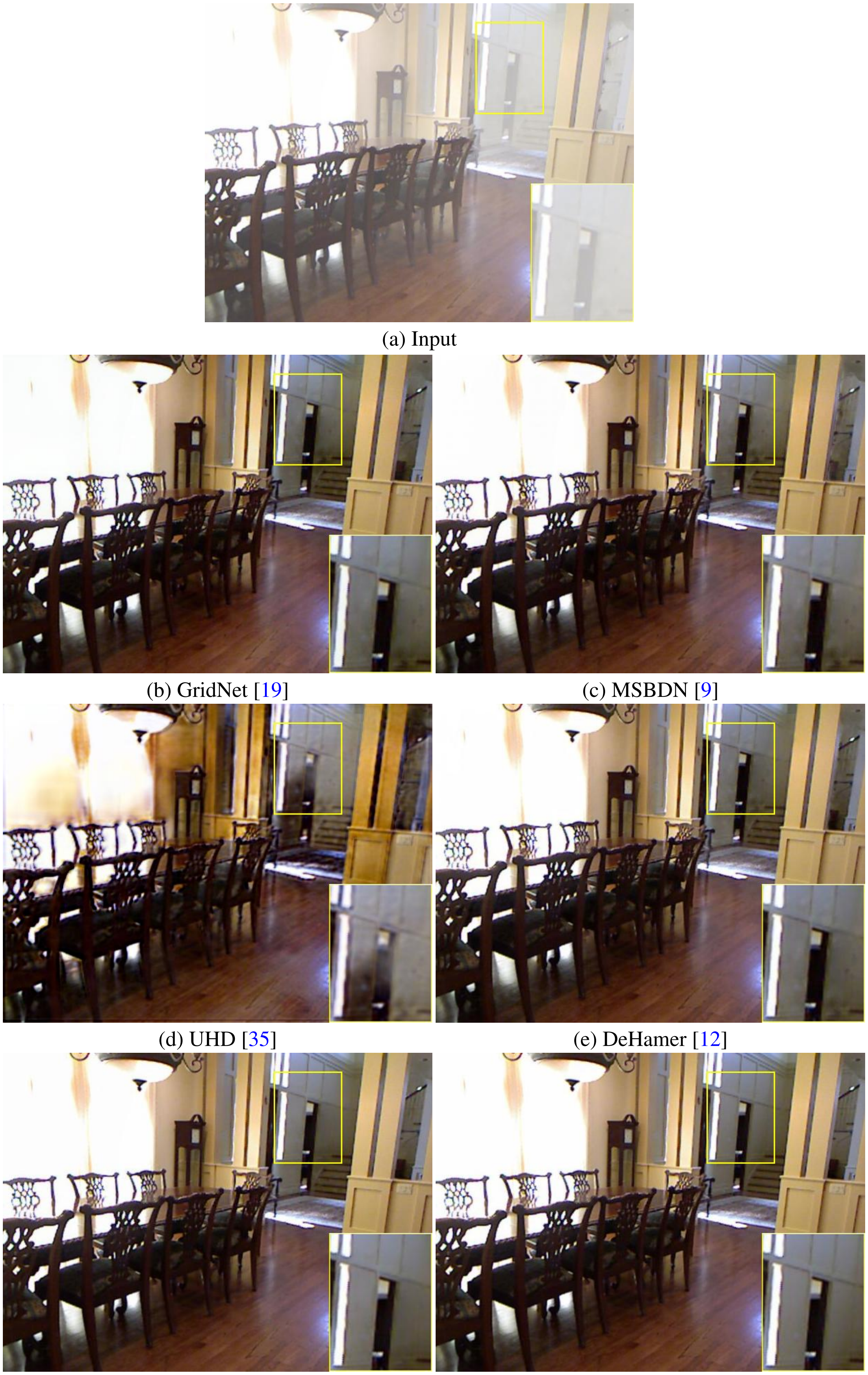

(a) Input

(b) GridNet [19]

(c) MSBDN [9]

(d) UHD [35]

(e) DeHamer [12]

(f) PromptRestorer

(g) GT

Figure 9: **Image dehazing** example on SOTS-Indoor [16].

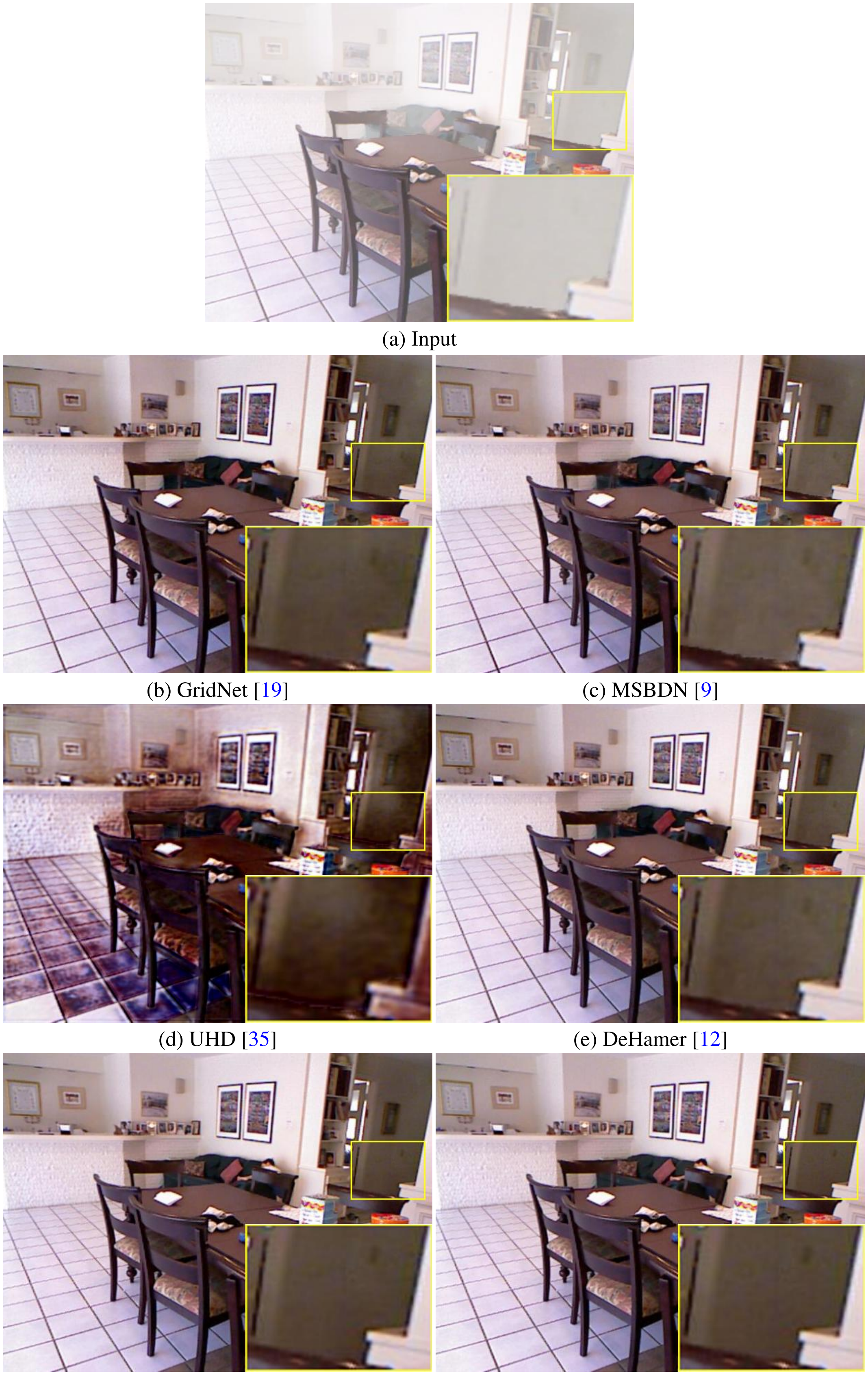

(a) Input

(b) GridNet [19]

(c) MSBDN [9]

(d) UHD [35]

(e) DeHamer [12]

(f) PromptRestorer

(g) GT

Figure 10: **Image dehazing** example on SOTS-Indoor [16].

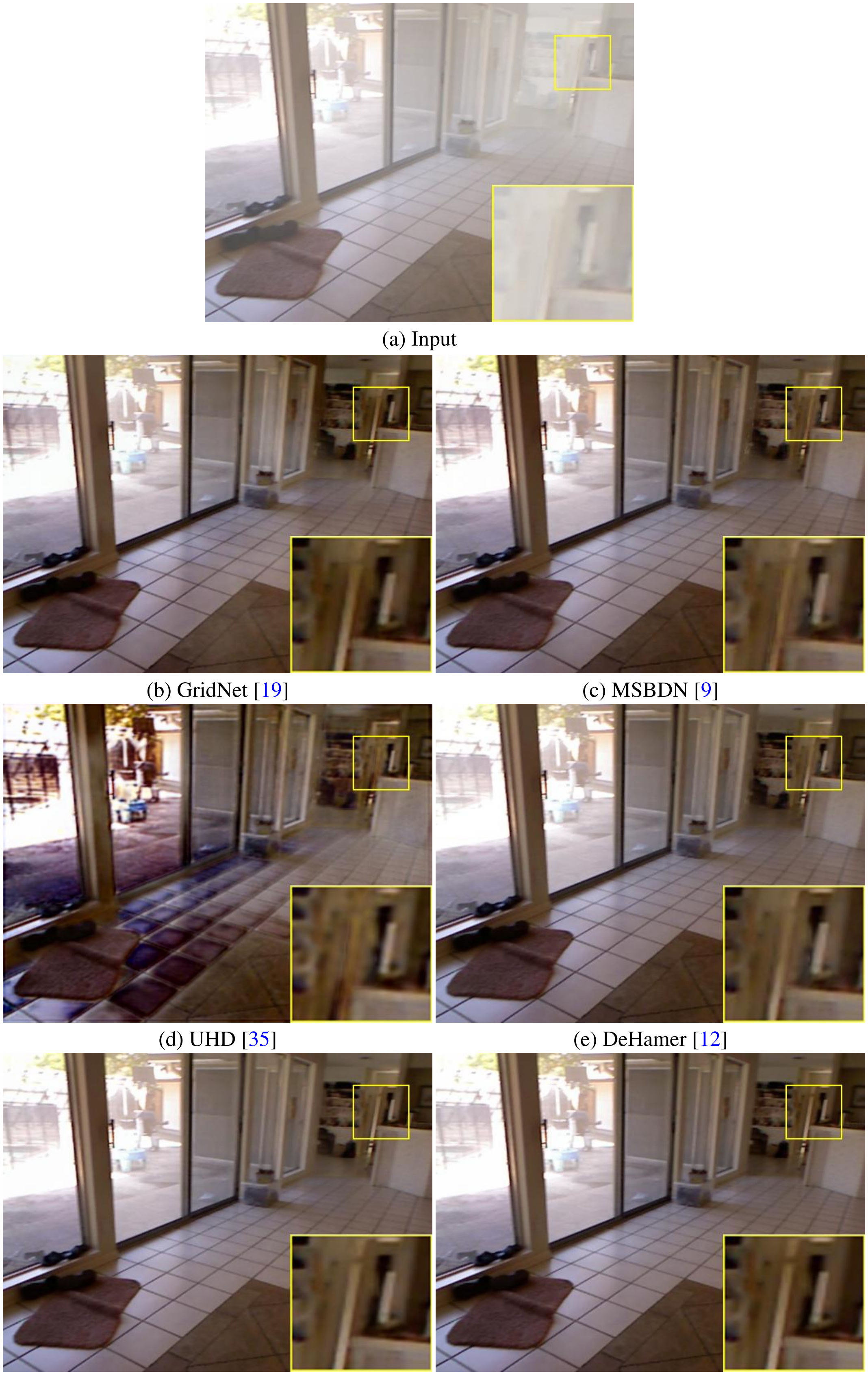

(a) Input

(b) GridNet [19]

(c) MSBDN [9]

(d) UHD [35]

(e) DeHamer [12]

(f) PromptRestorer

(g) GT

Figure 11: **Image dehazing** example on SOTS-Indoor [16].

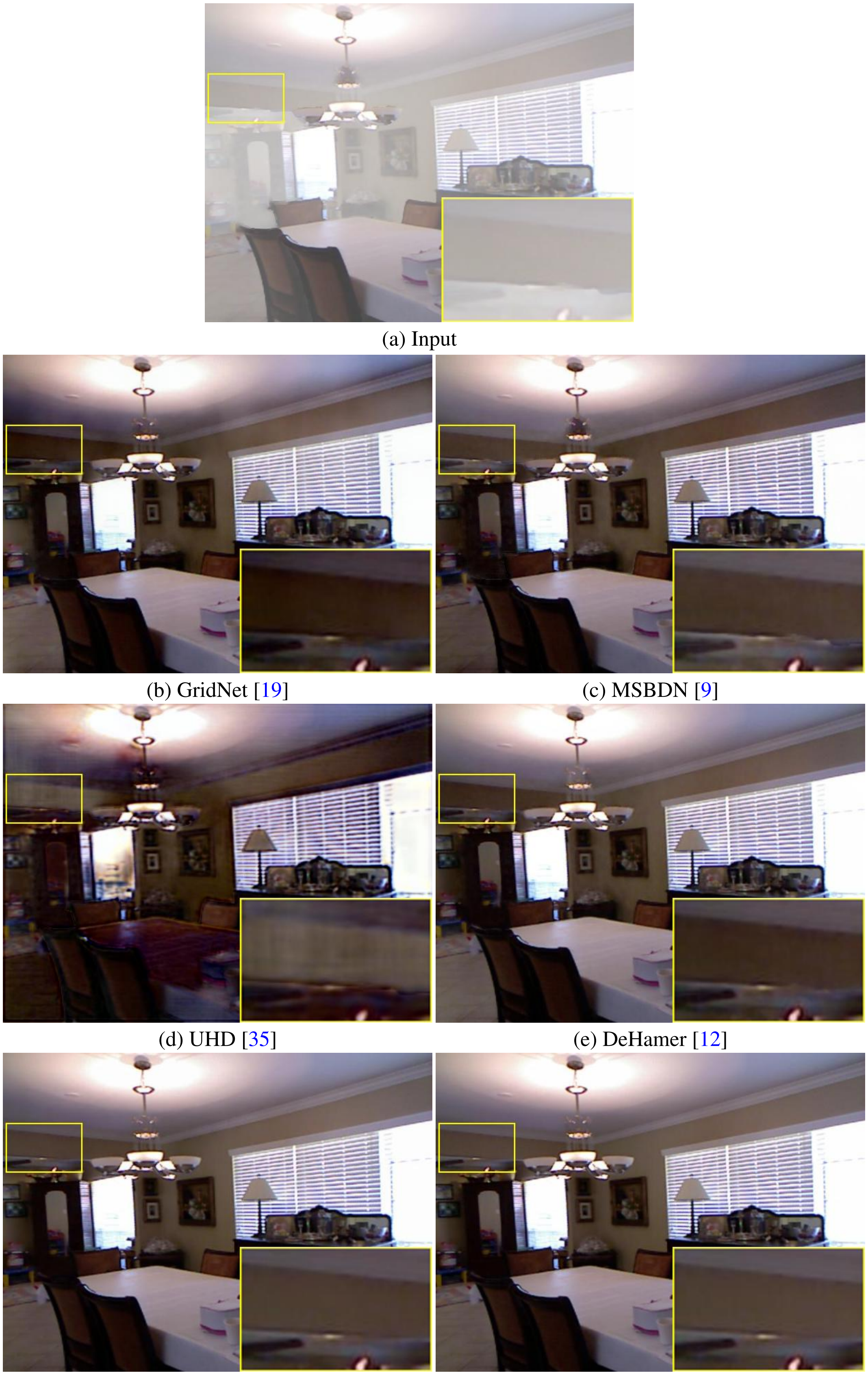

(a) Input

(b) GridNet [19]

(c) MSBDN [9]

(d) UHD [35]

(e) DeHamer [12]

(f) PromptRestorer

(g) GT

Figure 12: **Image dehazing** example on SOTS-Indoor [16].

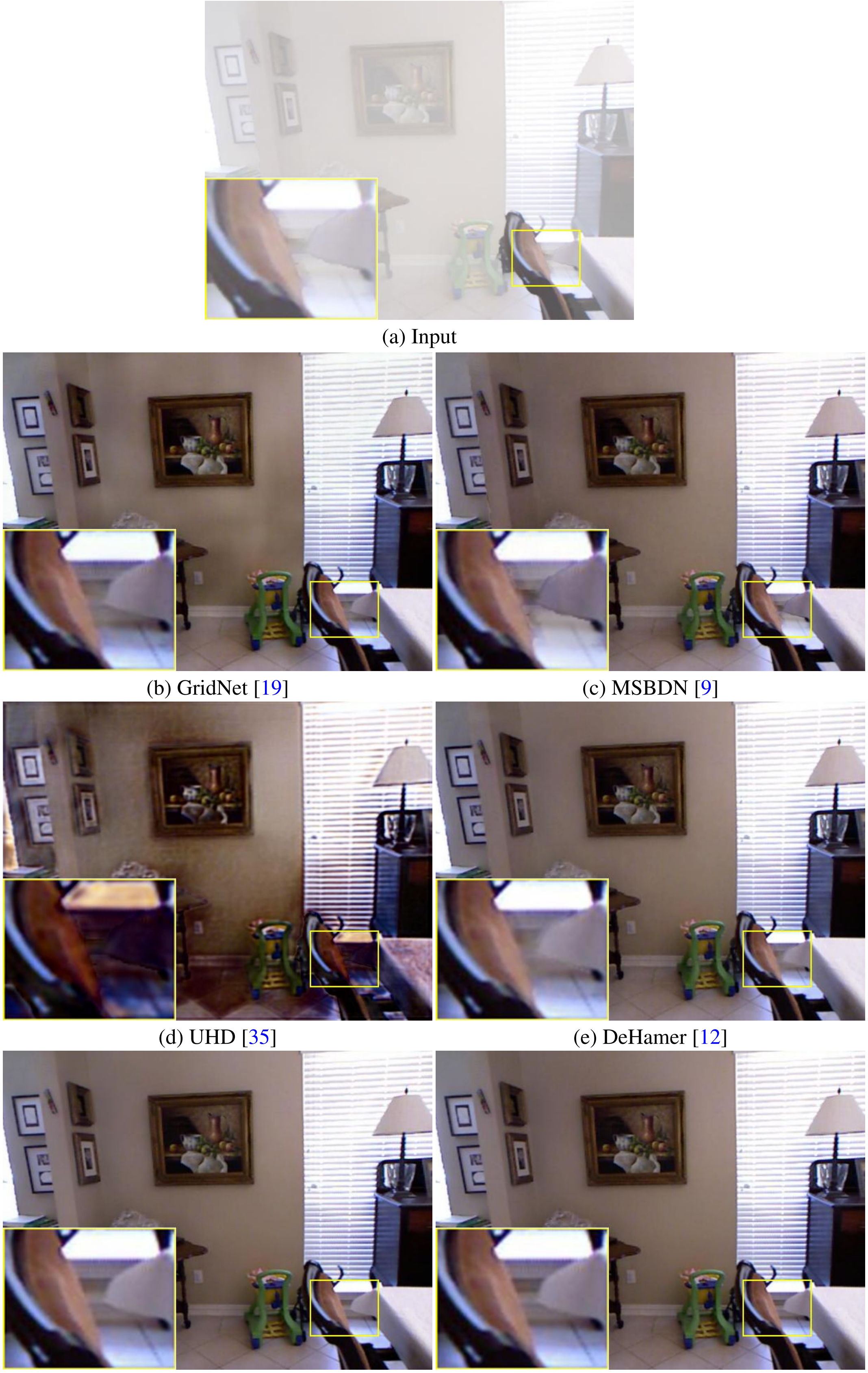

(a) Input

(b) GridNet [19]

(c) MSBDN [9]

(d) UHD [35]

(e) DeHamer [12]

(f) PromptRestorer

(g) GT

Figure 13: **Image dehazing** example on SOTS-Indoor [16].

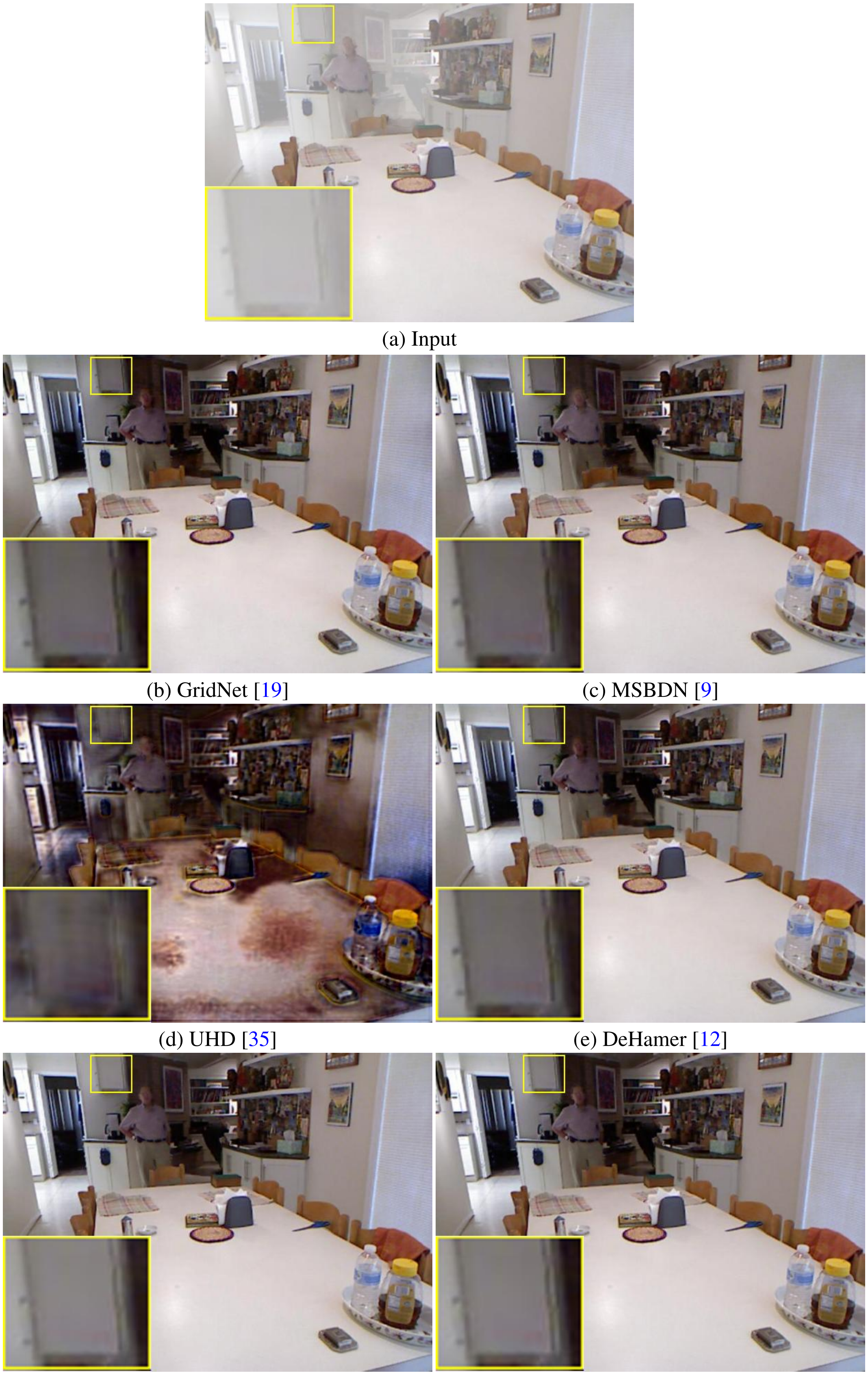

(a) Input

(b) GridNet [19]

(c) MSBDN [9]

(d) UHD [35]

(e) DeHamer [12]

(f) PromptRestorer

(g) GT

Figure 14: **Image dehazing** example on SOTS-Indoor [16].

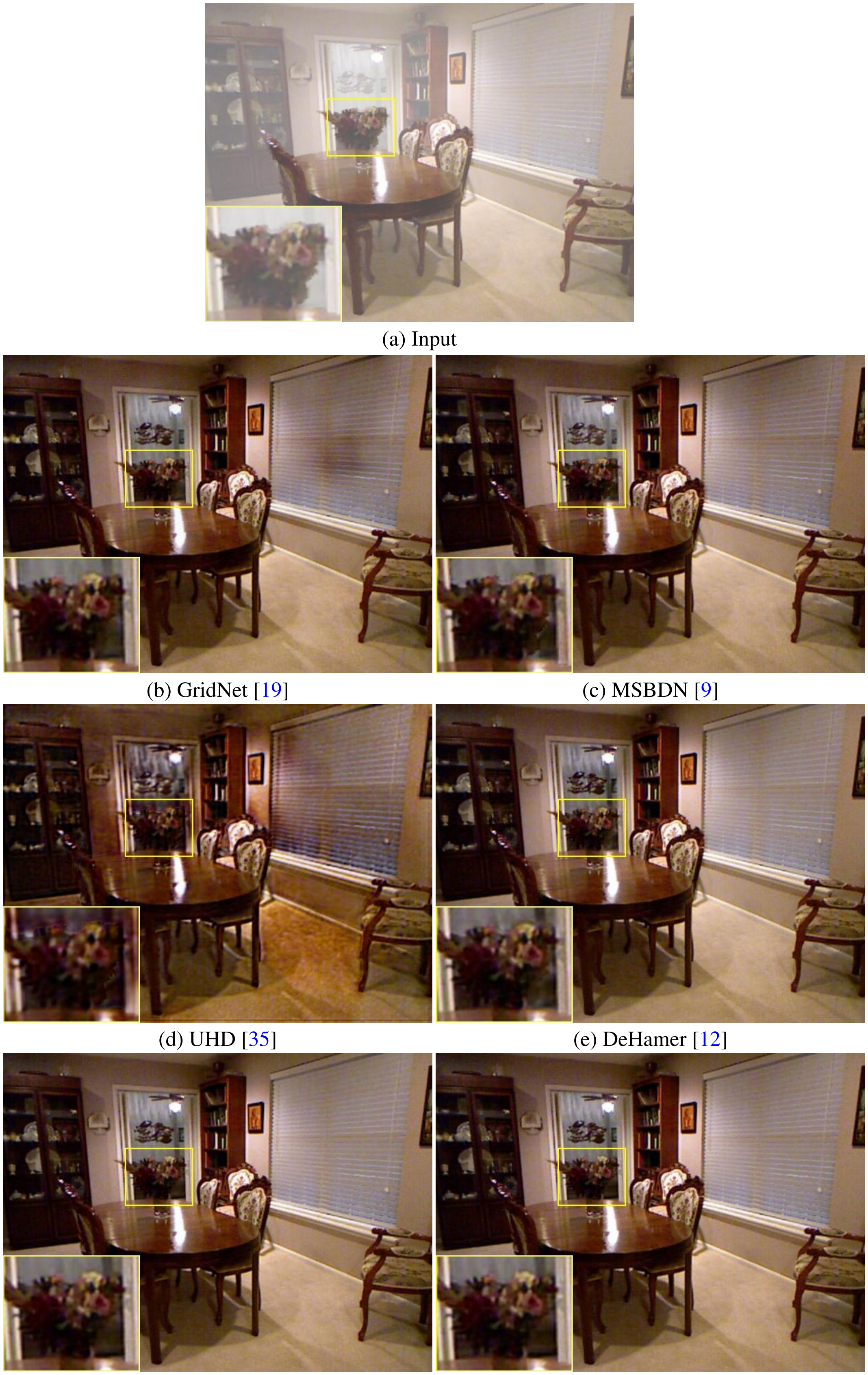

(a) Input

(b) GridNet [19]

(c) MSBDN [9]

(d) UHD [35]

(e) DeHamer [12]

(f) PromptRestorer

(g) GT

Figure 15: **Image dehazing** example on SOTS-Indoor [16].

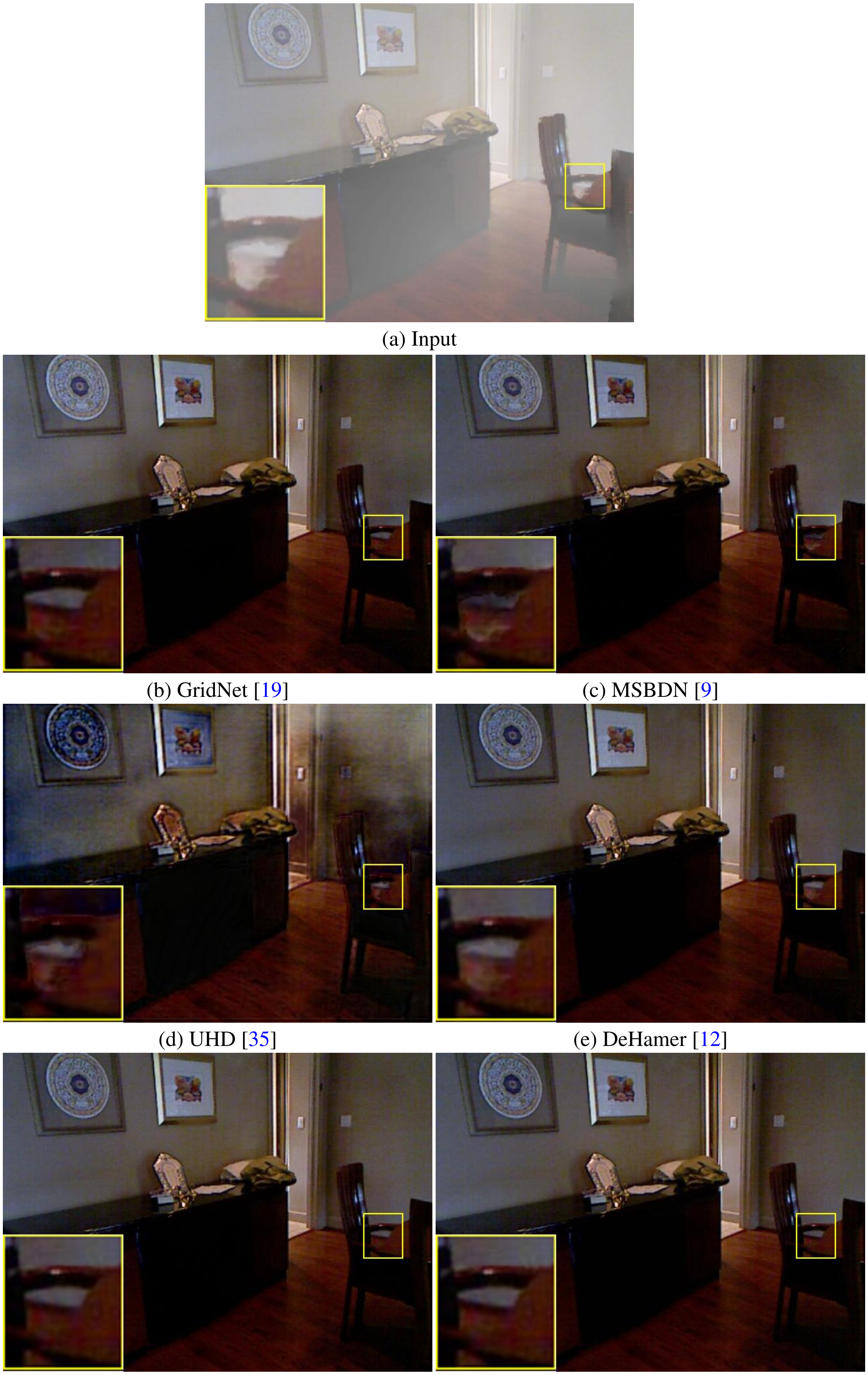

(a) Input

(b) GridNet [19]

(c) MSBDN [9]

(d) UHD [35]

(e) DeHamer [12]

(f) PromptRestorer

(g) GT

Figure 16: **Image dehazing** example on SOTS-Indoor [16].

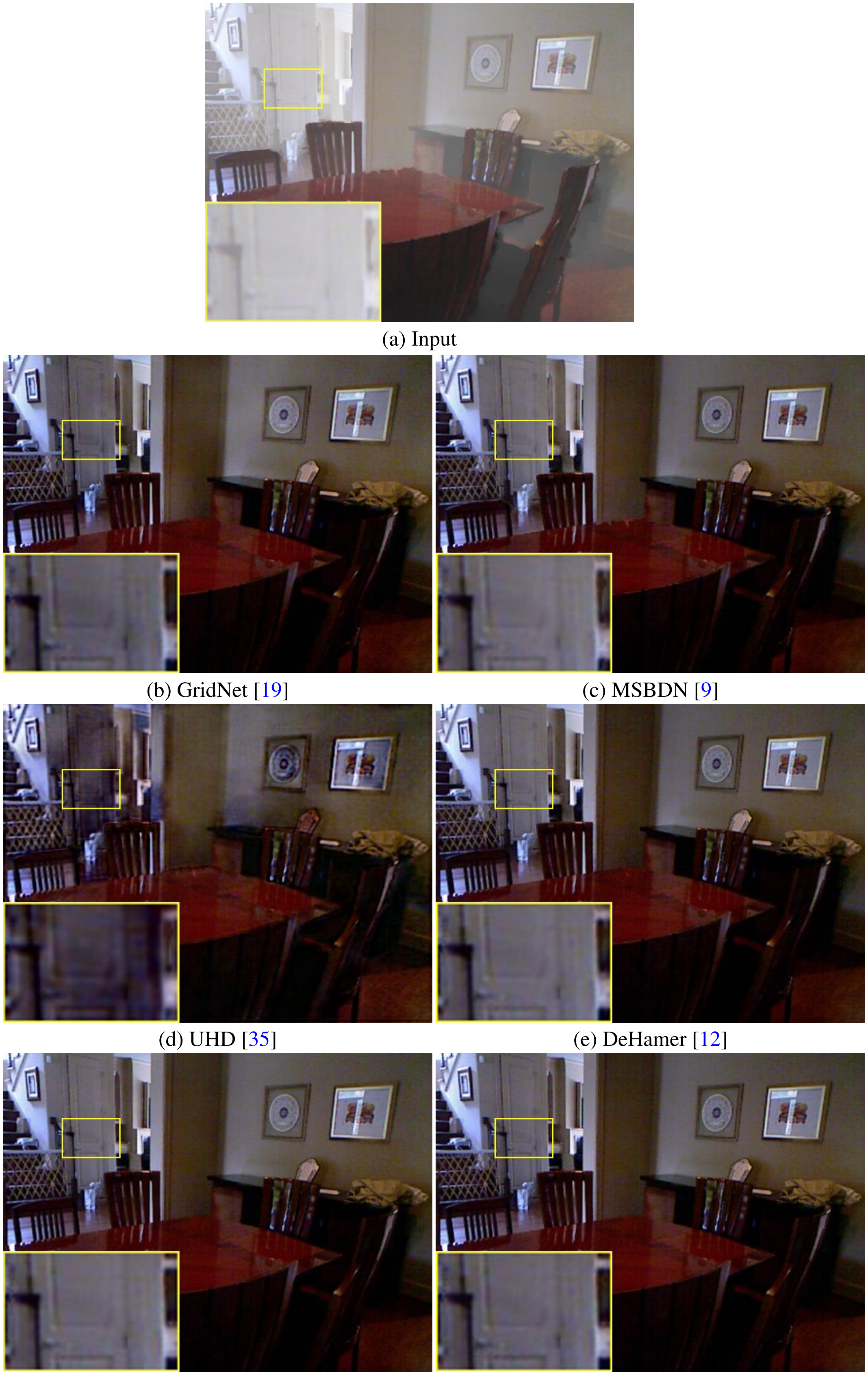

(a) Input

(b) GridNet [19]

(c) MSBDN [9]

(d) UHD [35]

(e) DeHamer [12]

(f) PromptRestorer

(g) GT

Figure 17: **Image dehazing** example on SOTS-Indoor [16].

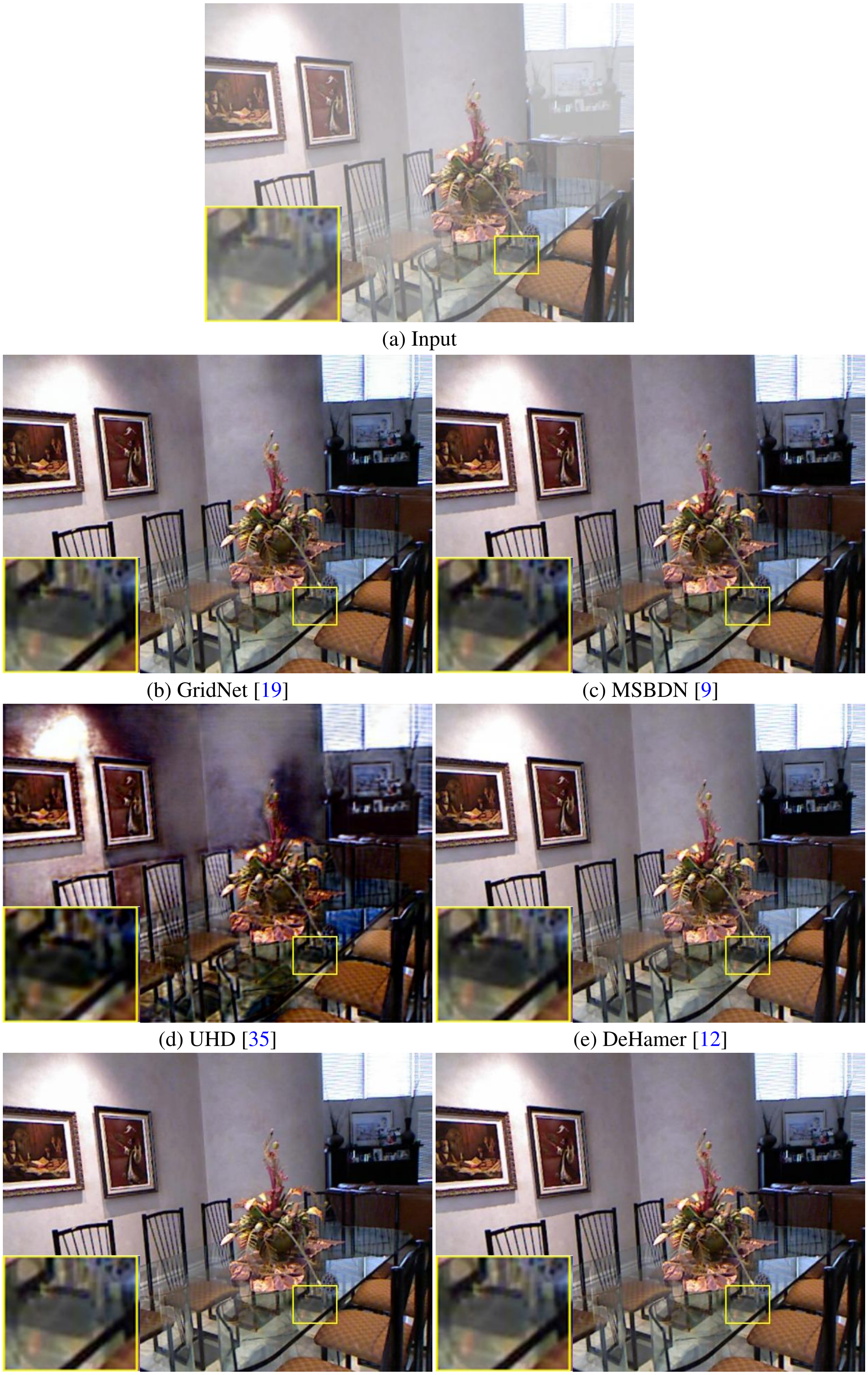

(a) Input

(b) GridNet [19]

(c) MSBDN [9]

(d) UHD [35]

(e) DeHamer [12]

(f) PromptRestorer

(g) GT

Figure 18: **Image dehazing** example on SOTS-Indoor [16].

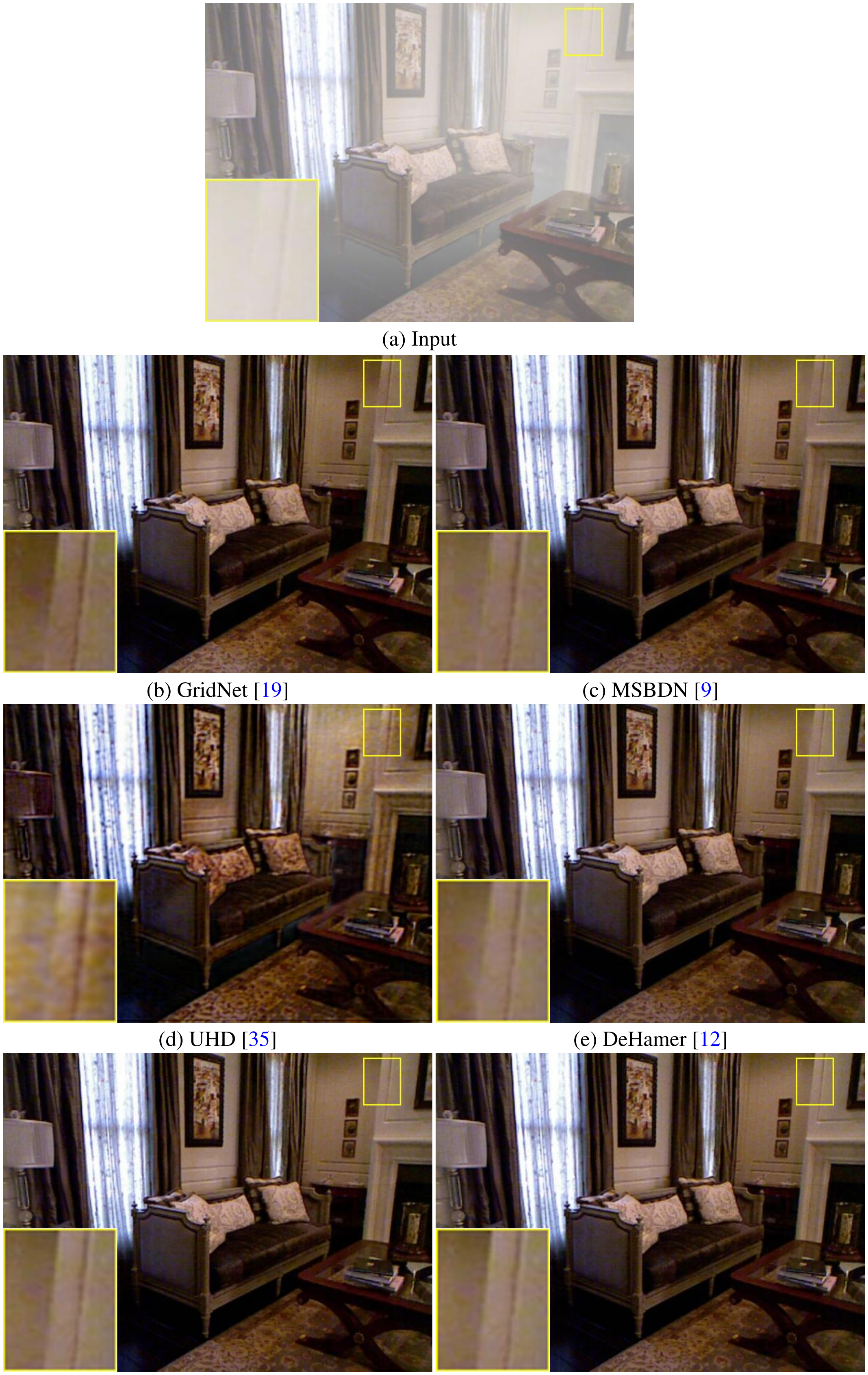

(a) Input

(b) GridNet [19]

(c) MSBDN [9]

(d) UHD [35]

(e) DeHamer [12]

(f) PromptRestorer

(g) GT

Figure 19: **Image dehazing** example on SOTS-Indoor [16].

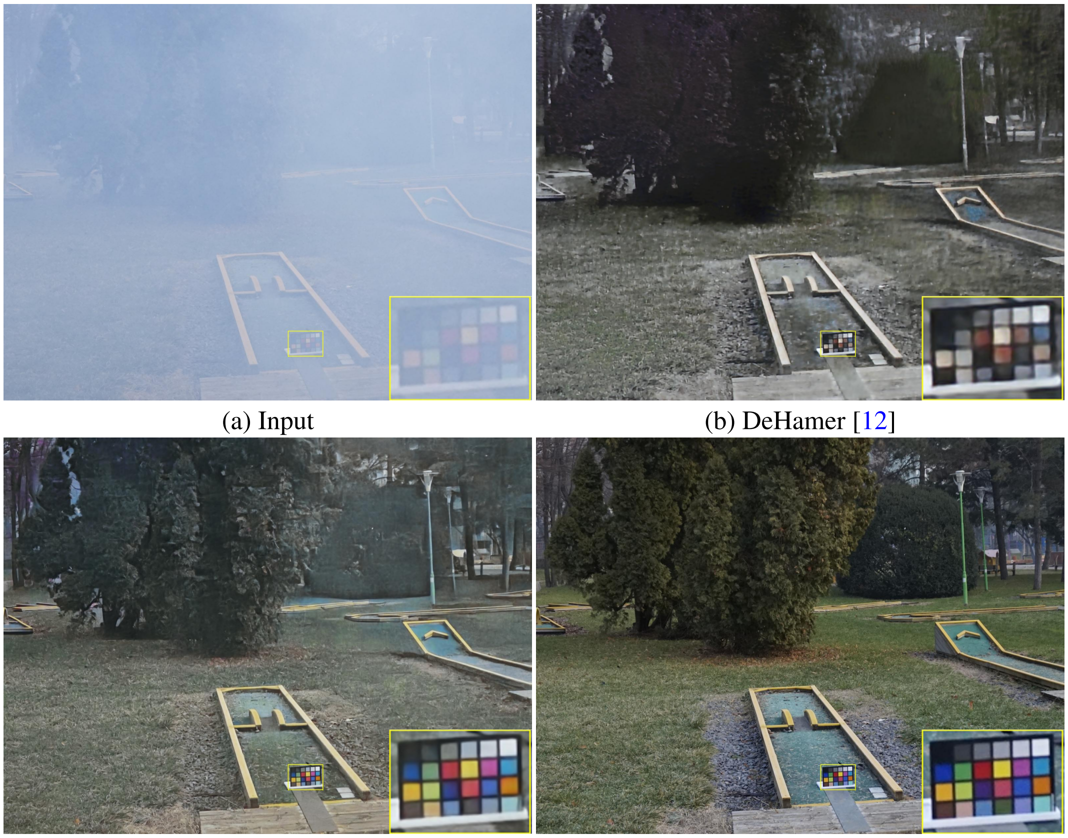

(a) Input

(b) DeHamer [12]

(c) PromptRestorer

(d) GT

Figure 20: **Image dehazing** example on Dense-Haze [1].

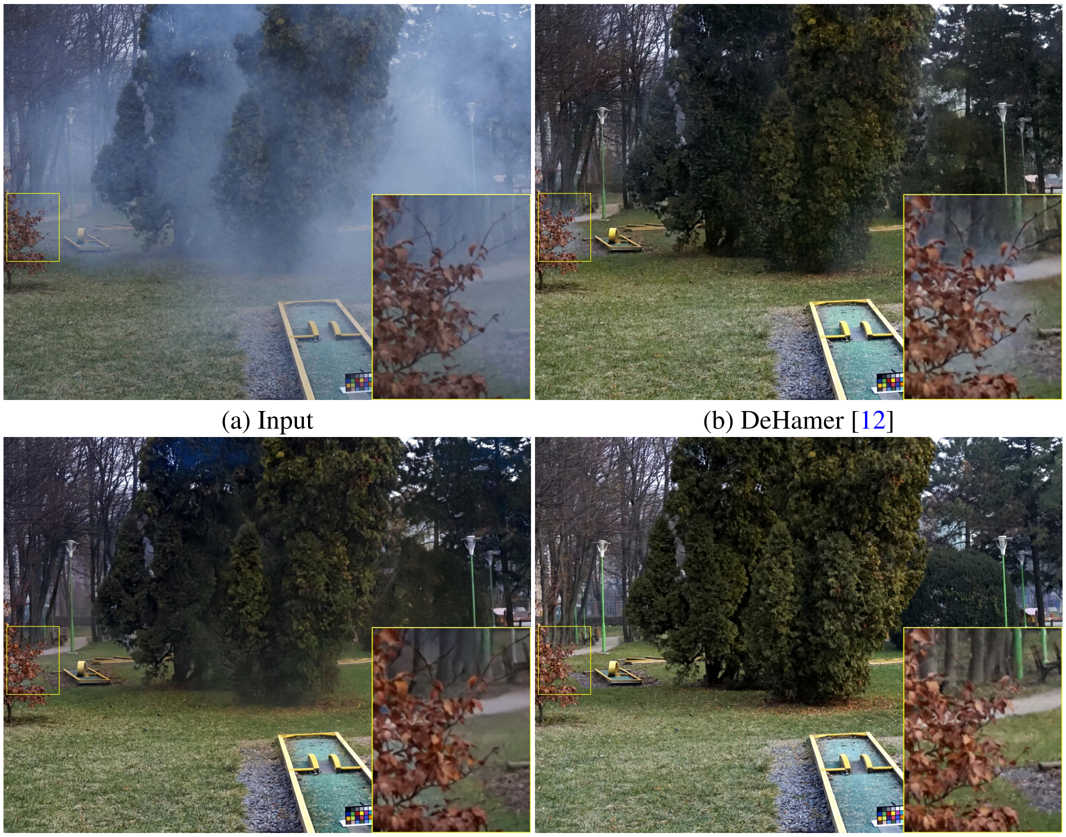

(a) Input

(b) DeHamer [12]

(c) PromptRestorer

(d) GT

Figure 21: **Image dehazing** example on NH-Haze [2].

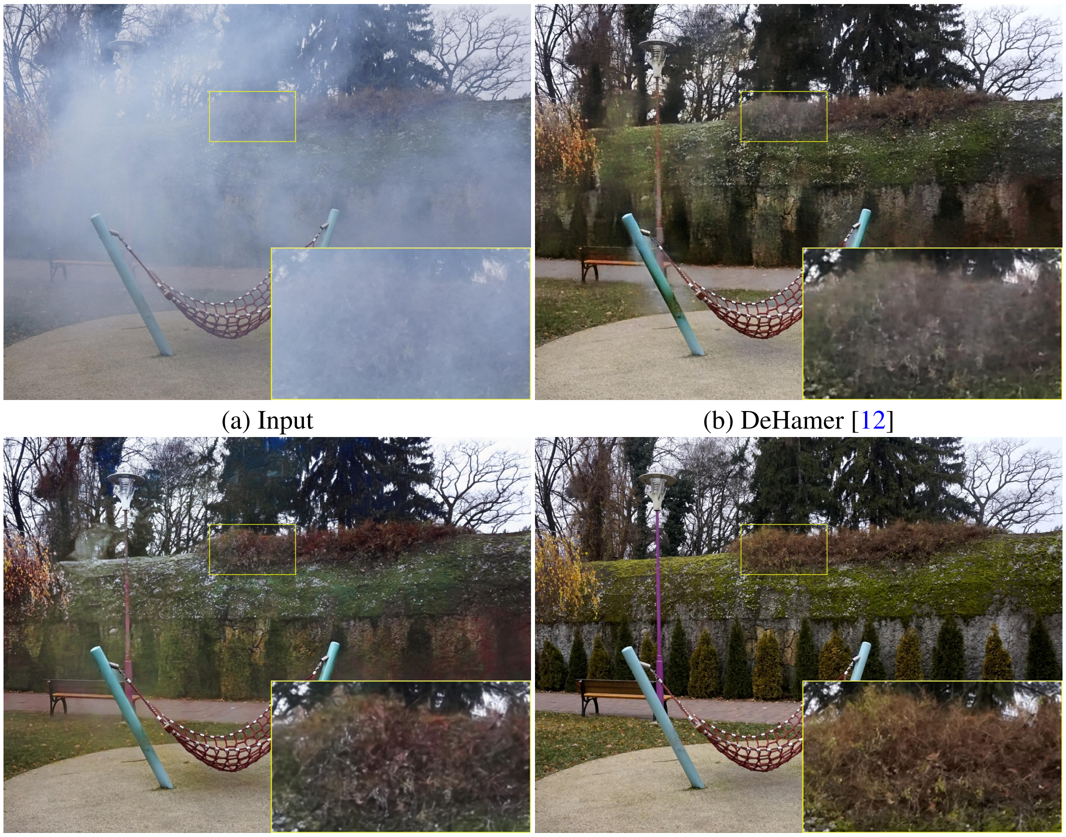

(a) Input

(b) DeHamer [12]

(c) PromptRestorer

(d) GT

Figure 22: **Image dehazing** example on NH-Haze [2].

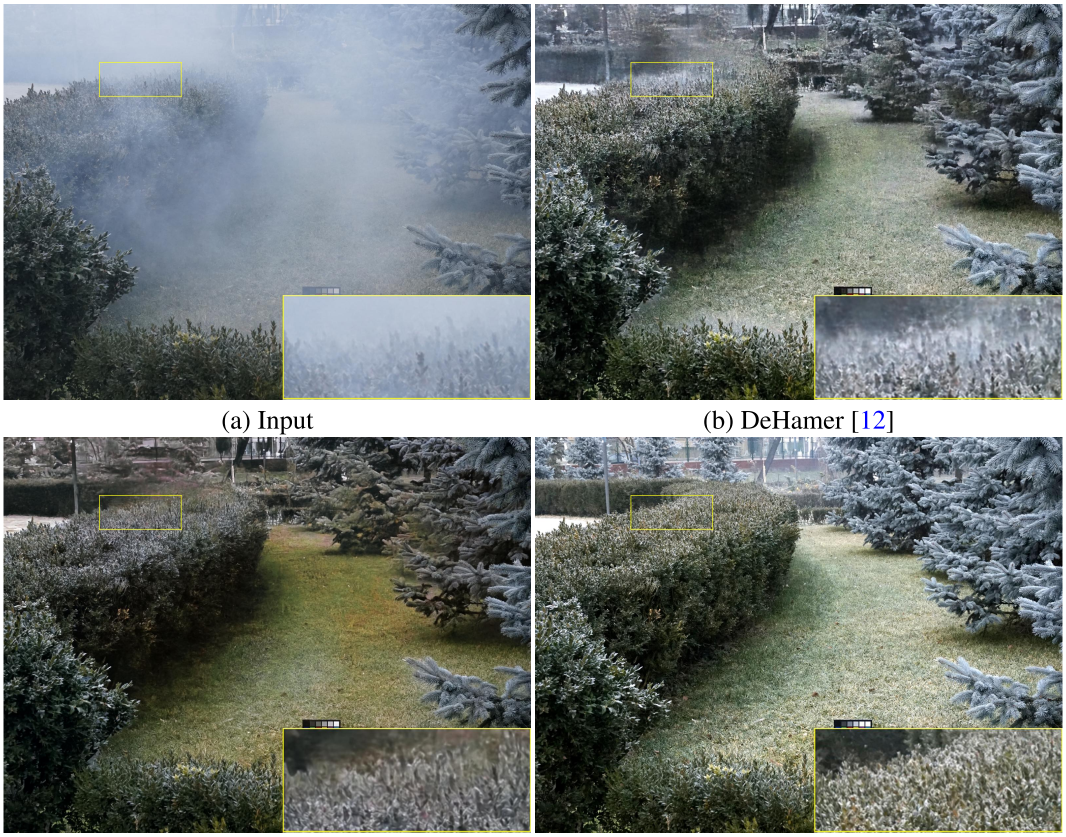

(a) Input

(b) DeHamer [12]

(c) PromptRestorer

(d) GT

Figure 23: **Image dehazing** example on NH-Haze [2].

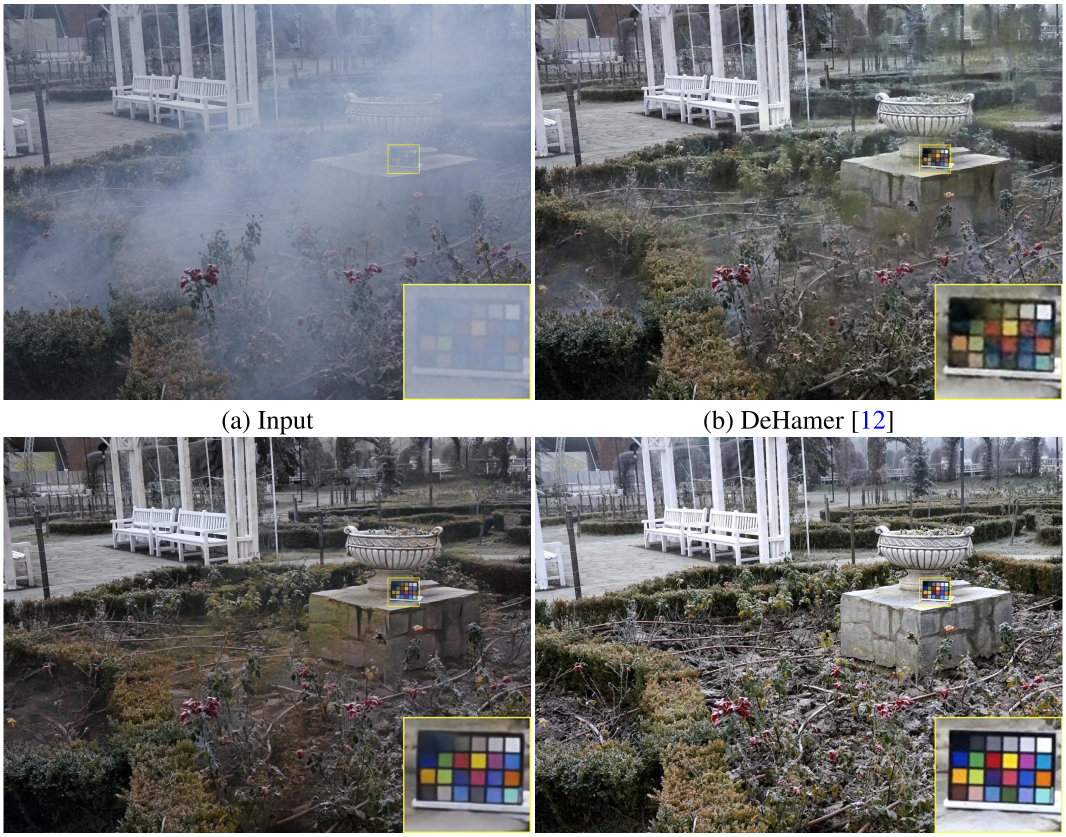

(a) Input

(b) DeHamer [12]

(c) PromptRestorer

(d) GT

Figure 24: **Image dehazing** example on NH-Haze [2].

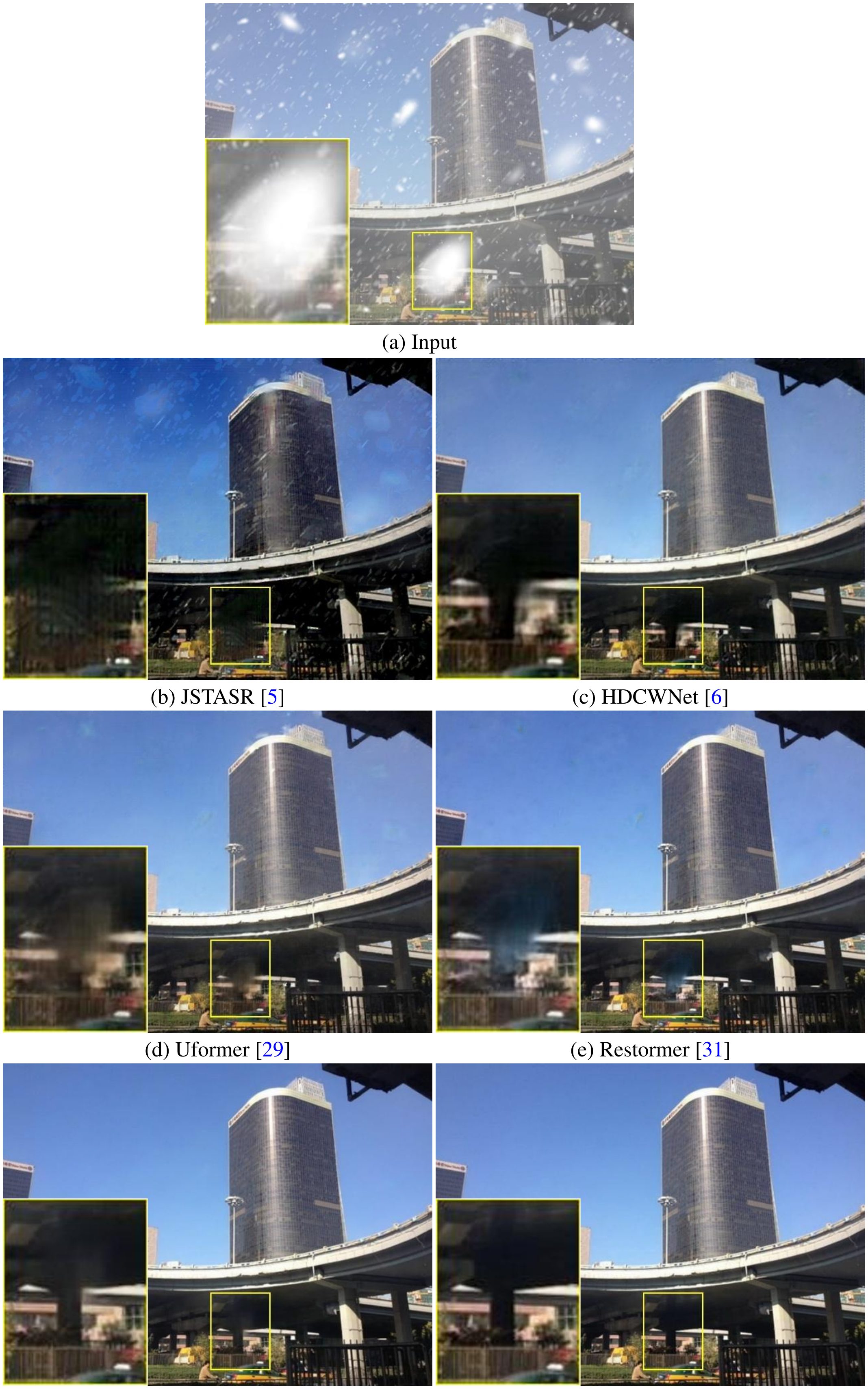

(a) Input

(b) JSTASR [5]

(c) HDCWNet [6]

(d) Uformer [29]

(e) Restormer [31]

(f) PromptRestorer

(g) GT

Figure 25: **Image desnowing** example on CSD (2000) [6].

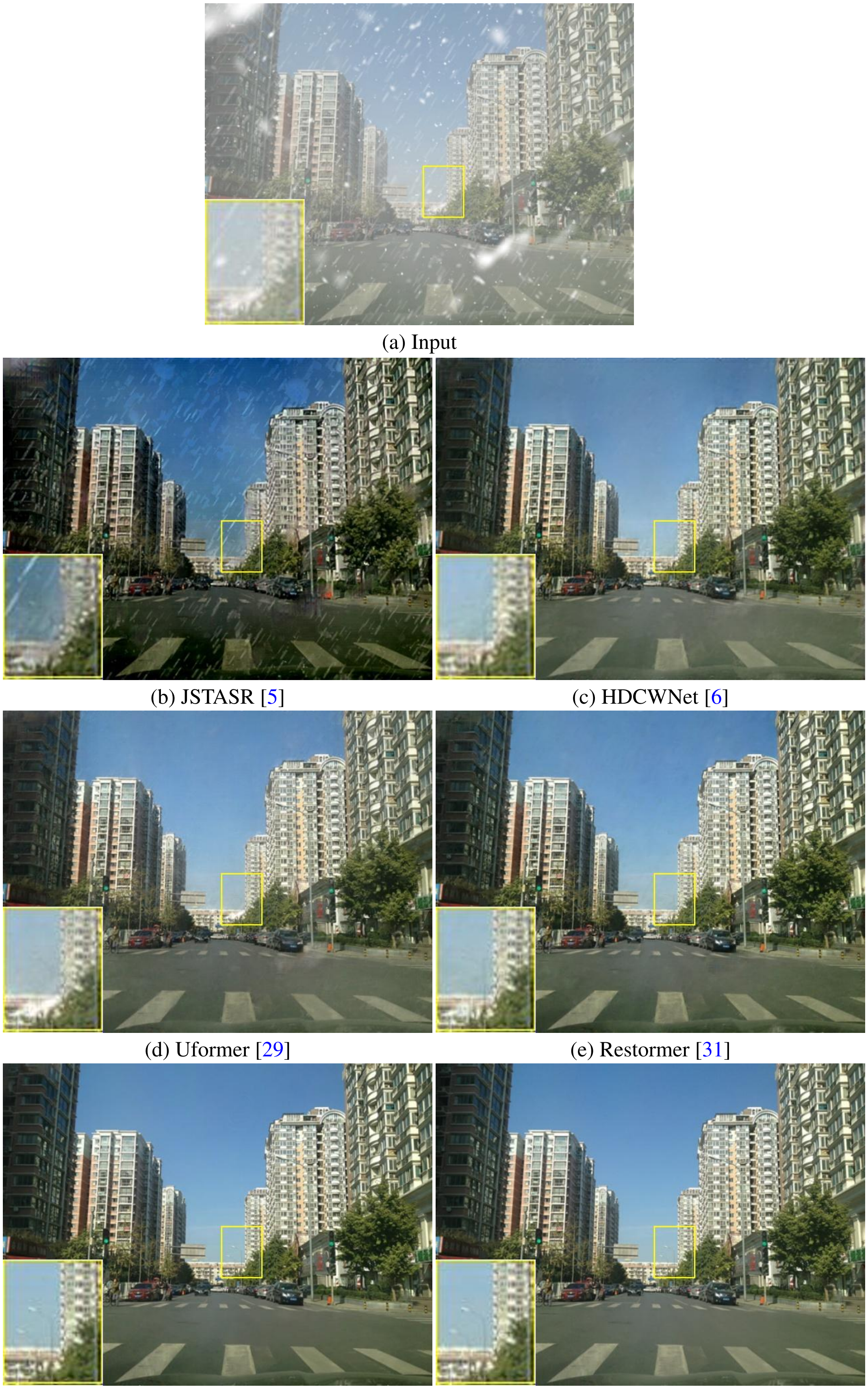

(a) Input

(b) JSTASR [5]

(c) HDCWNet [6]

(d) Uformer [29]

(e) Restormer [31]

(f) PromptRestorer

(g) GT

Figure 26: **Image desnowing** example on CSD (2000) [6].

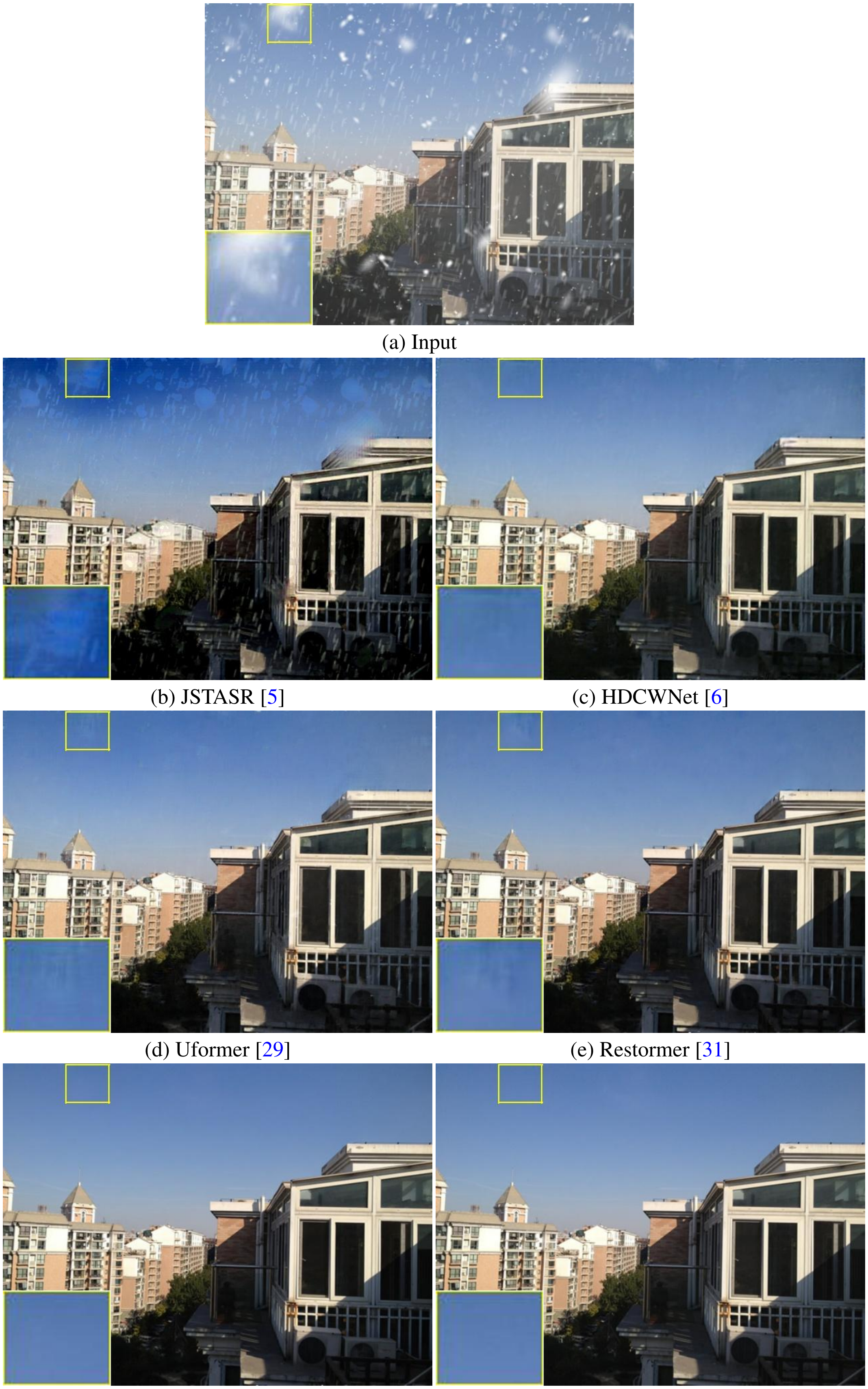

(a) Input

(b) JSTASR [5]

(c) HDCWNet [6]

(d) Uformer [29]

(e) Restormer [31]

(f) PromptRestorer

(g) GT

Figure 27: **Image desnowing** example on CSD (2000) [6].

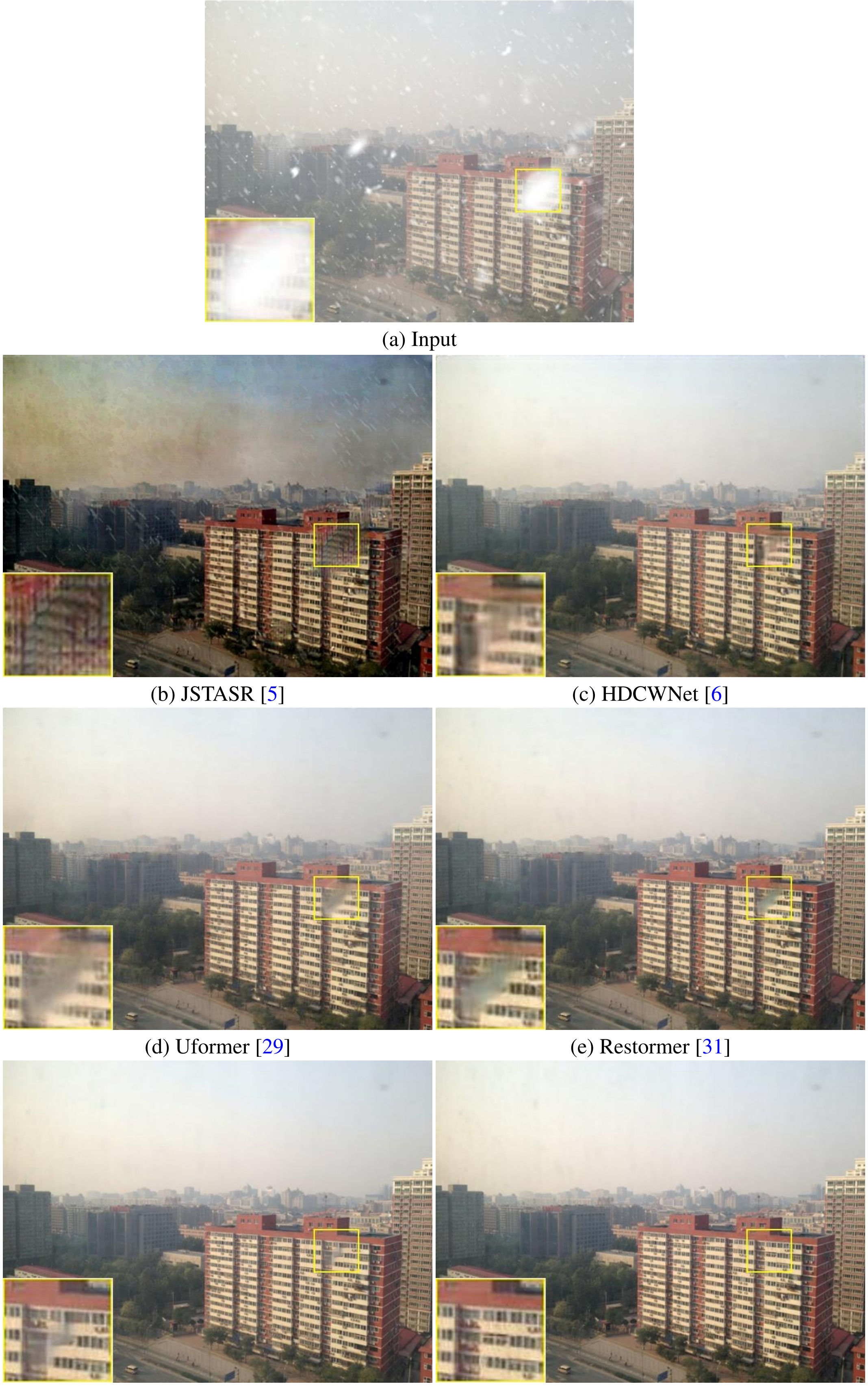

(a) Input

(b) JSTASR [5]

(c) HDCWNet [6]

(d) Uformer [29]

(e) Restormer [31]

(f) PromptRestorer

(g) GT

Figure 28: **Image desnowing** example on CSD (2000) [6].

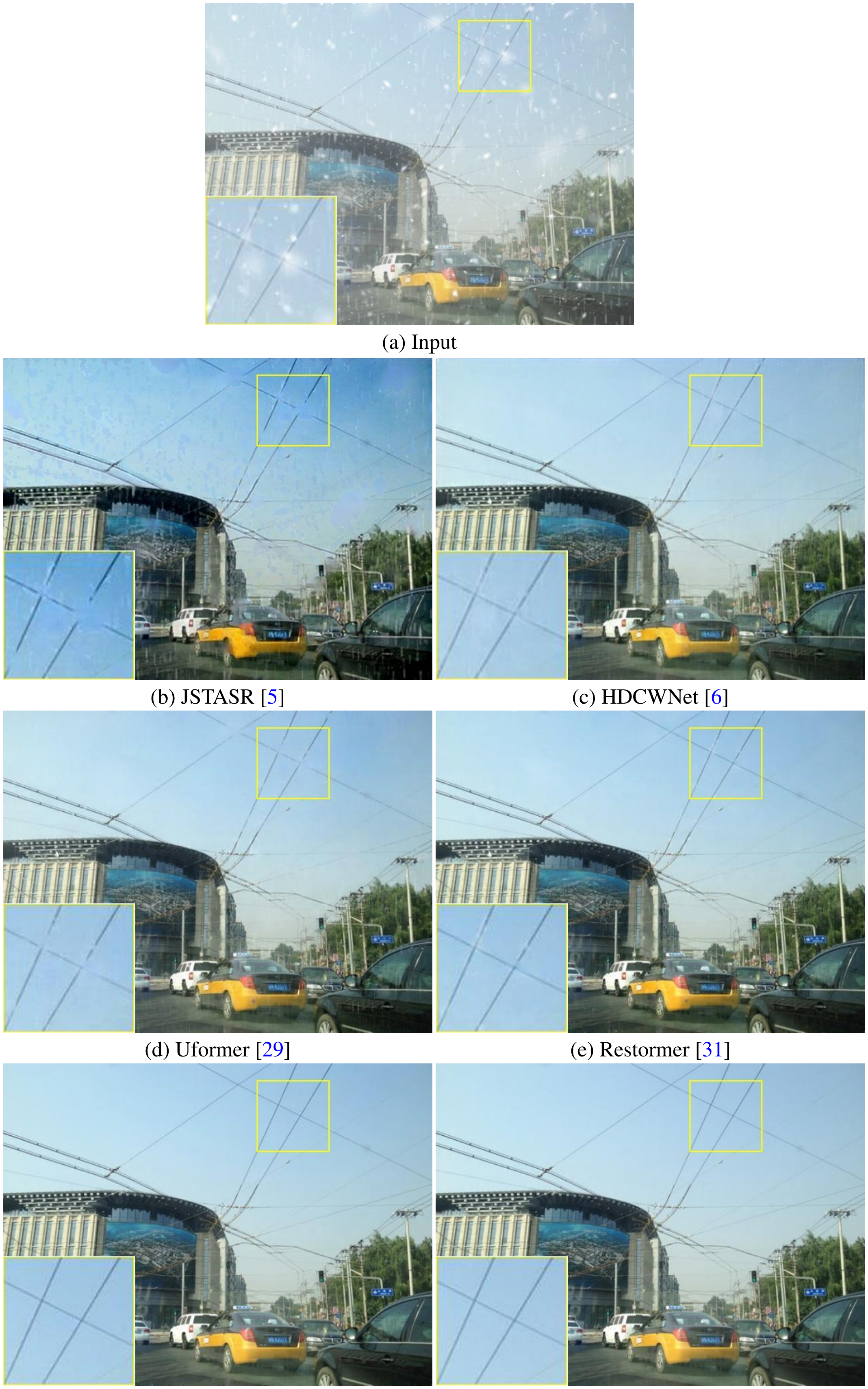

(a) Input

(b) JSTASR [5]

(c) HDCWNet [6]

(d) Uformer [29]

(e) Restormer [31]

(f) PromptRestorer

(g) GT

Figure 29: **Image desnowing** example on CSD (2000) [6].

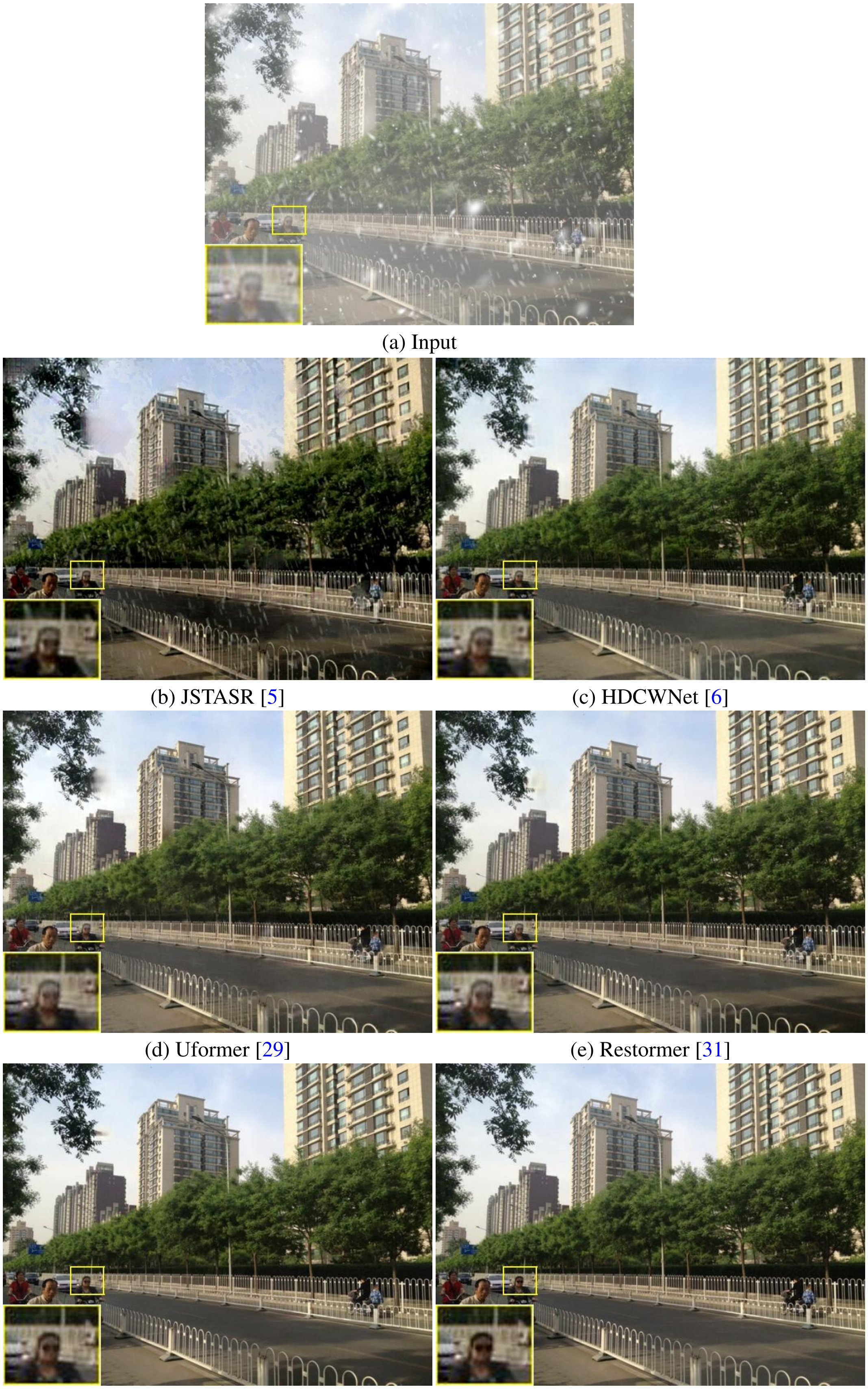

(a) Input

(b) JSTASR [5]

(c) HDCWNet [6]

(d) Uformer [29]

(e) Restormer [31]

(f) PromptRestorer

(g) GT

Figure 30: **Image desnowing** example on CSD (2000) [6].

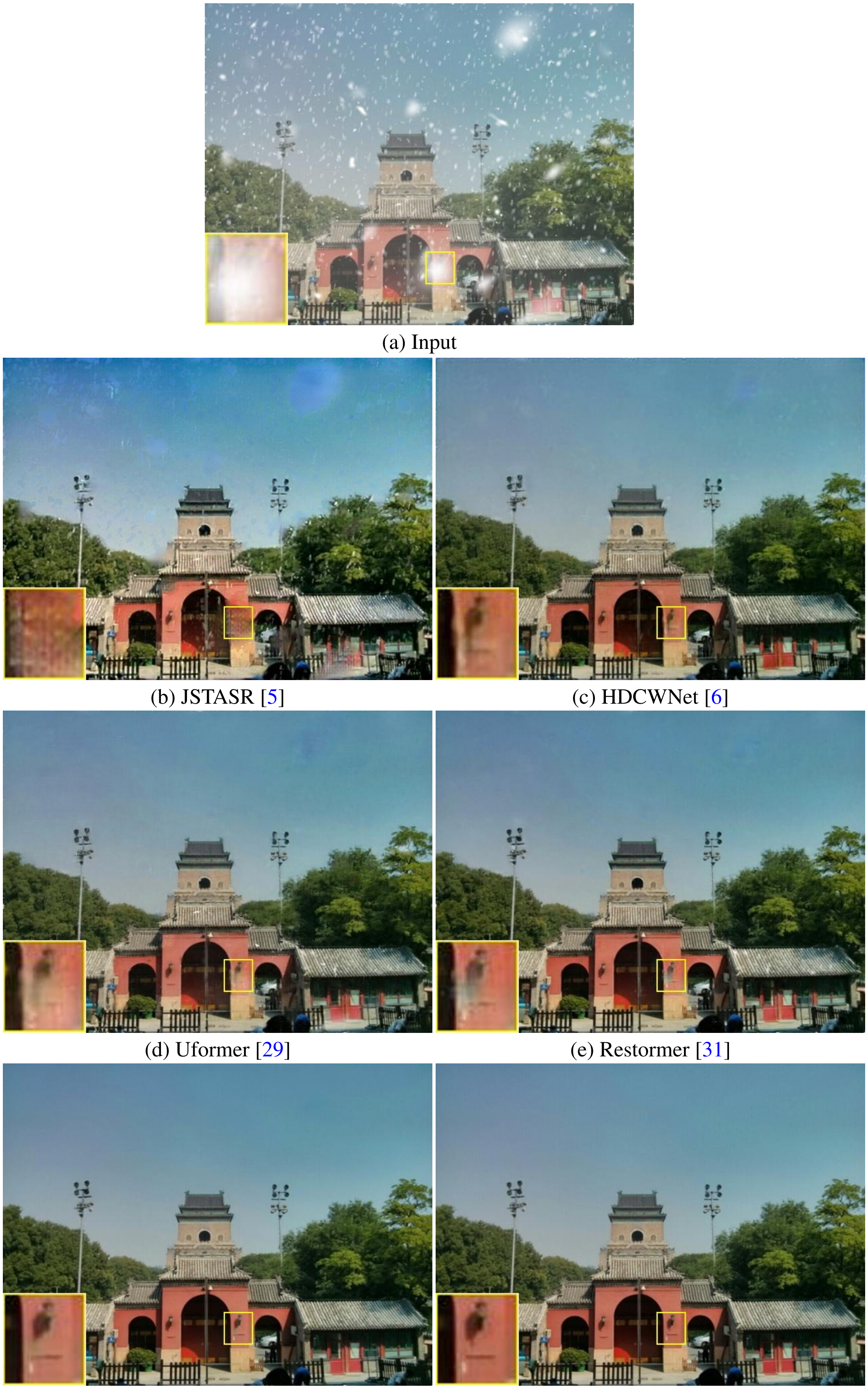

(a) Input

(b) JSTASR [5]

(c) HDCWNet [6]

(d) Uformer [29]

(e) Restormer [31]

(f) PromptRestorer

(g) GT

Figure 31: **Image desnowing** example on CSD (2000) [6].

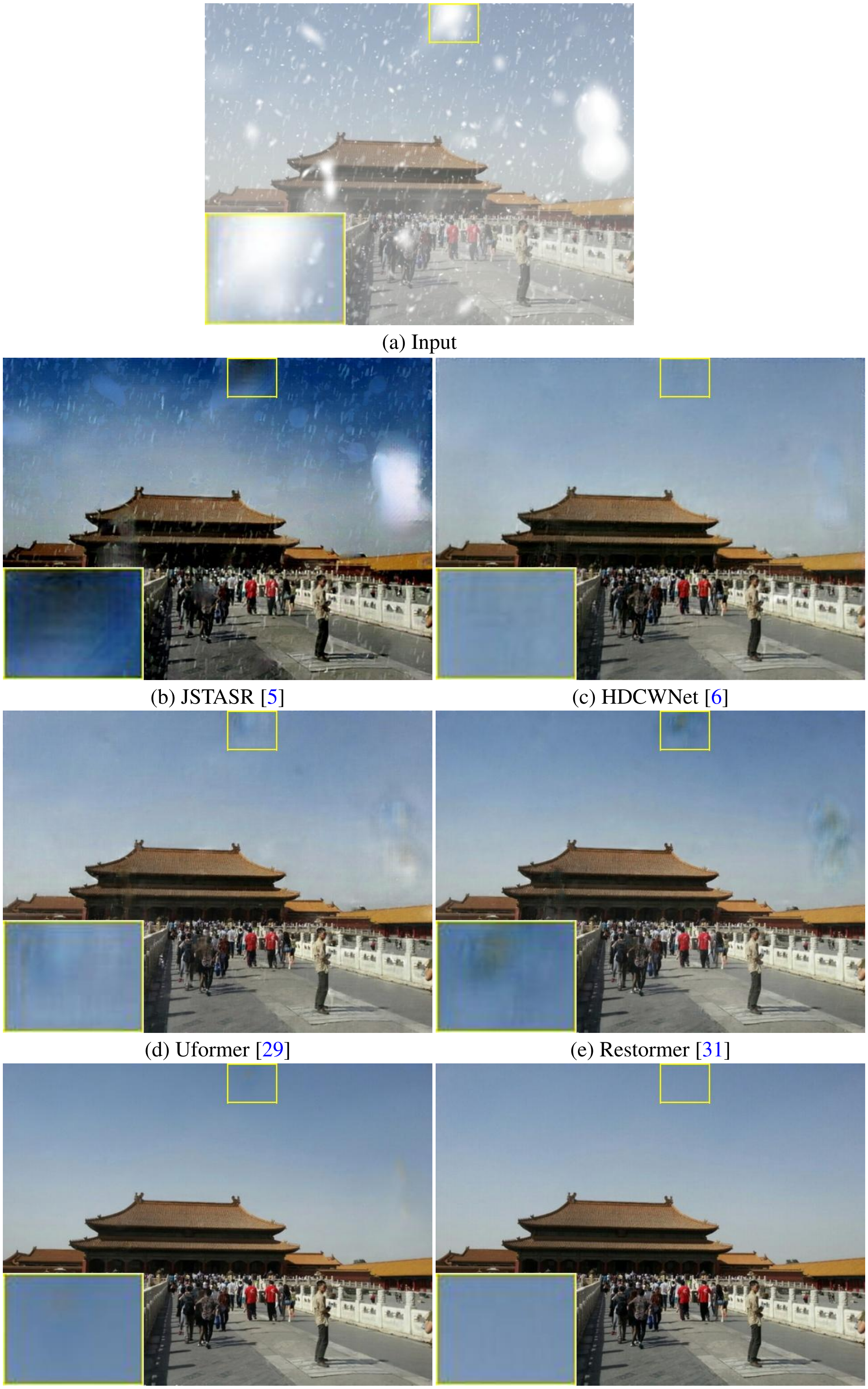

(a) Input

(b) JSTASR [5]

(c) HDCWNet [6]

(d) Uformer [29]

(e) Restormer [31]

(f) PromptRestorer

(g) GT

Figure 32: **Image desnowing** example on CSD (2000) [6].

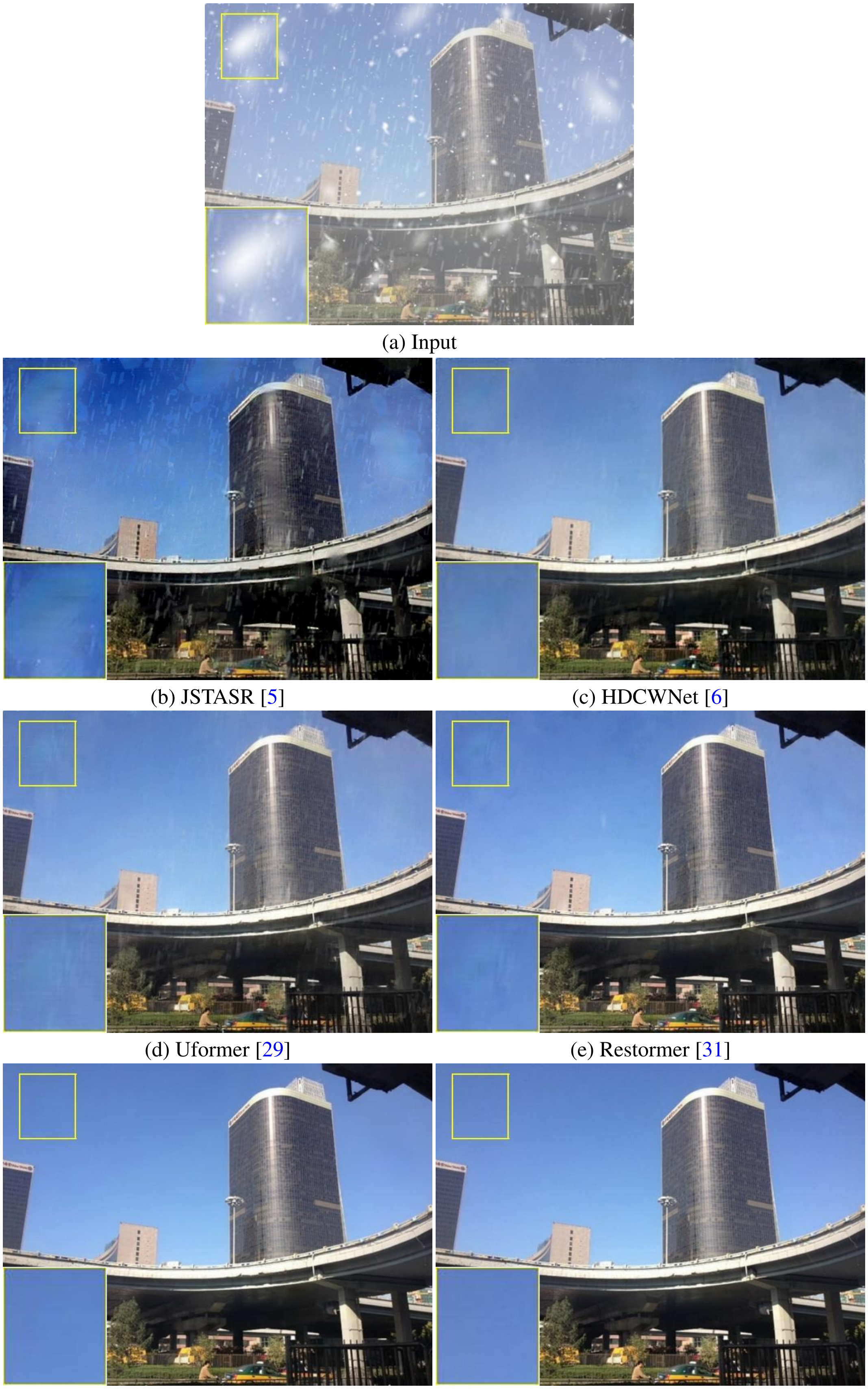

(a) Input

(b) JSTASR [5]

(c) HDCWNet [6]

(d) Uformer [29]

(e) Restormer [31]

(f) PromptRestorer

(g) GT

Figure 33: **Image desnowing** example on CSD (2000) [6].

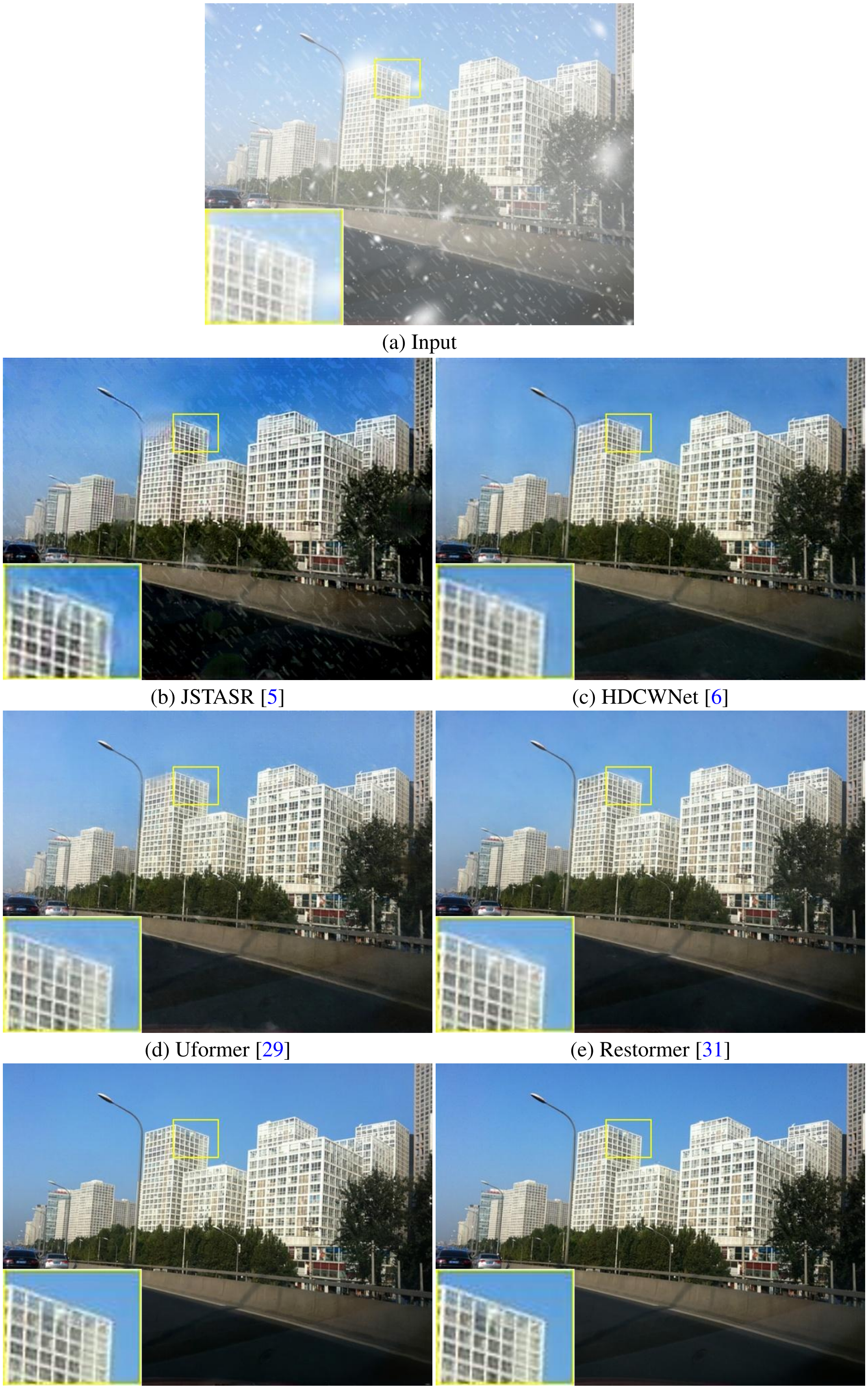

(a) Input

(b) JSTASR [5]

(c) HDCWNet [6]

(d) Uformer [29]

(e) Restormer [31]

(f) PromptRestorer

(g) GT

Figure 34: **Image desnowing** example on CSD (2000) [6].

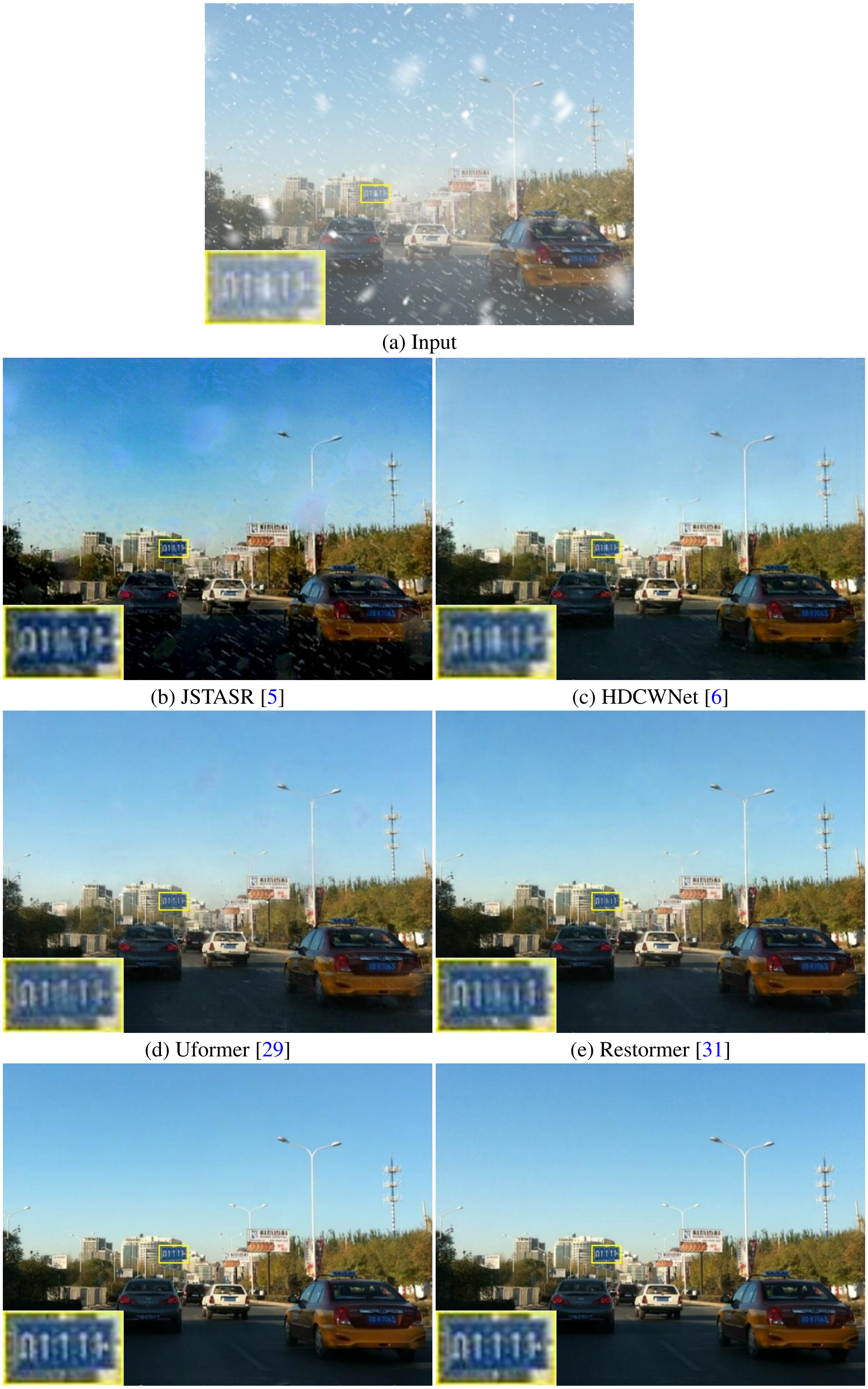

(a) Input

(b) JSTASR [5]

(c) HDCWNet [6]

(d) Uformer [29]

(e) Restormer [31]

(f) PromptRestorer

(g) GT

Figure 35: **Image desnowing** example on CSD (2000) [6].

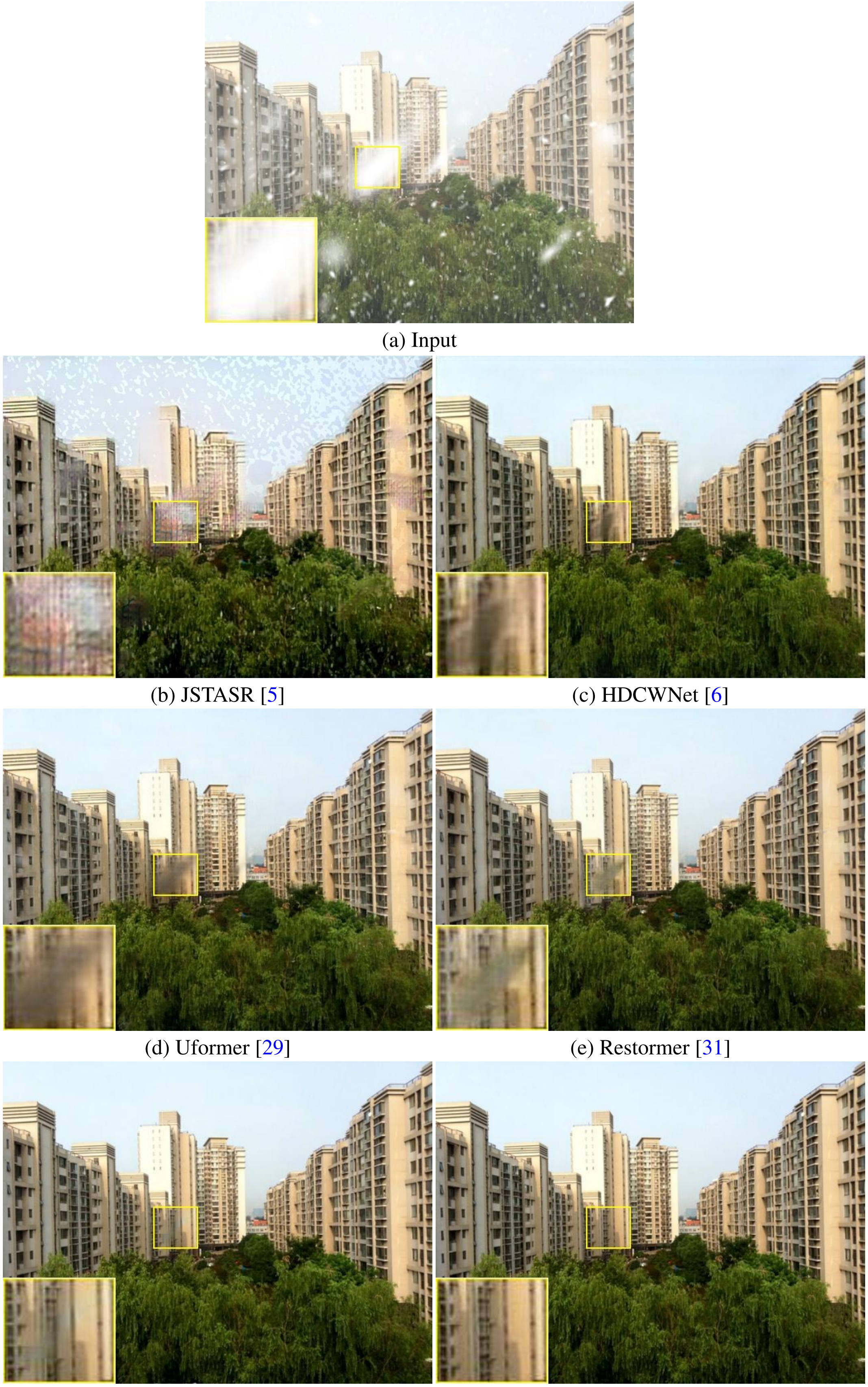

(a) Input

(b) JSTASR [5]

(c) HDCWNet [6]

(d) Uformer [29]

(e) Restormer [31]

(f) PromptRestorer

(g) GT

Figure 36: **Image desnowing** example on CSD (2000) [6].

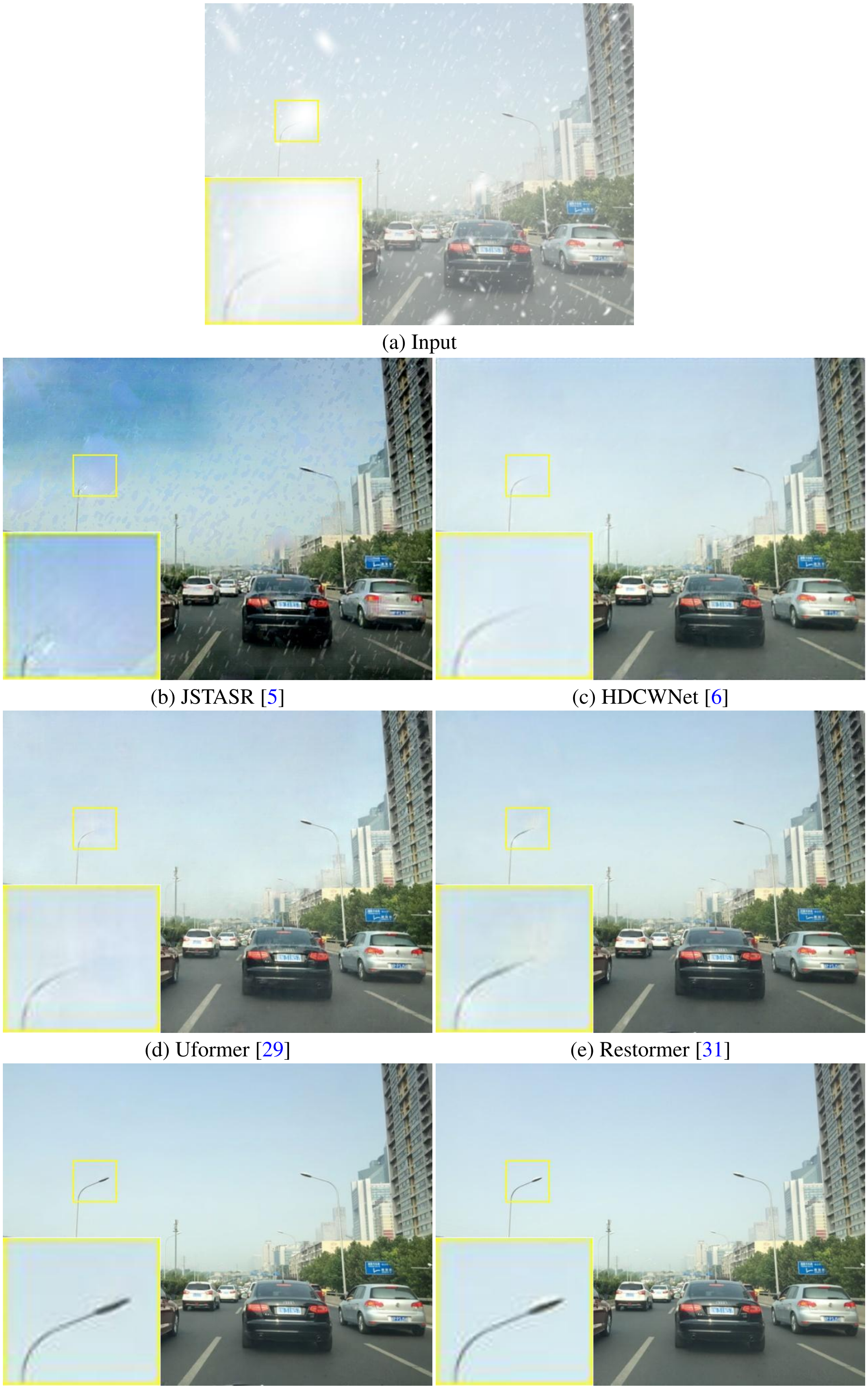

(a) Input

(b) JSTASR [5]

(c) HDCWNet [6]

(d) Uformer [29]

(e) Restormer [31]

(f) PromptRestorer

(g) GT

Figure 37: **Image desnowing** example on CSD (2000) [6].

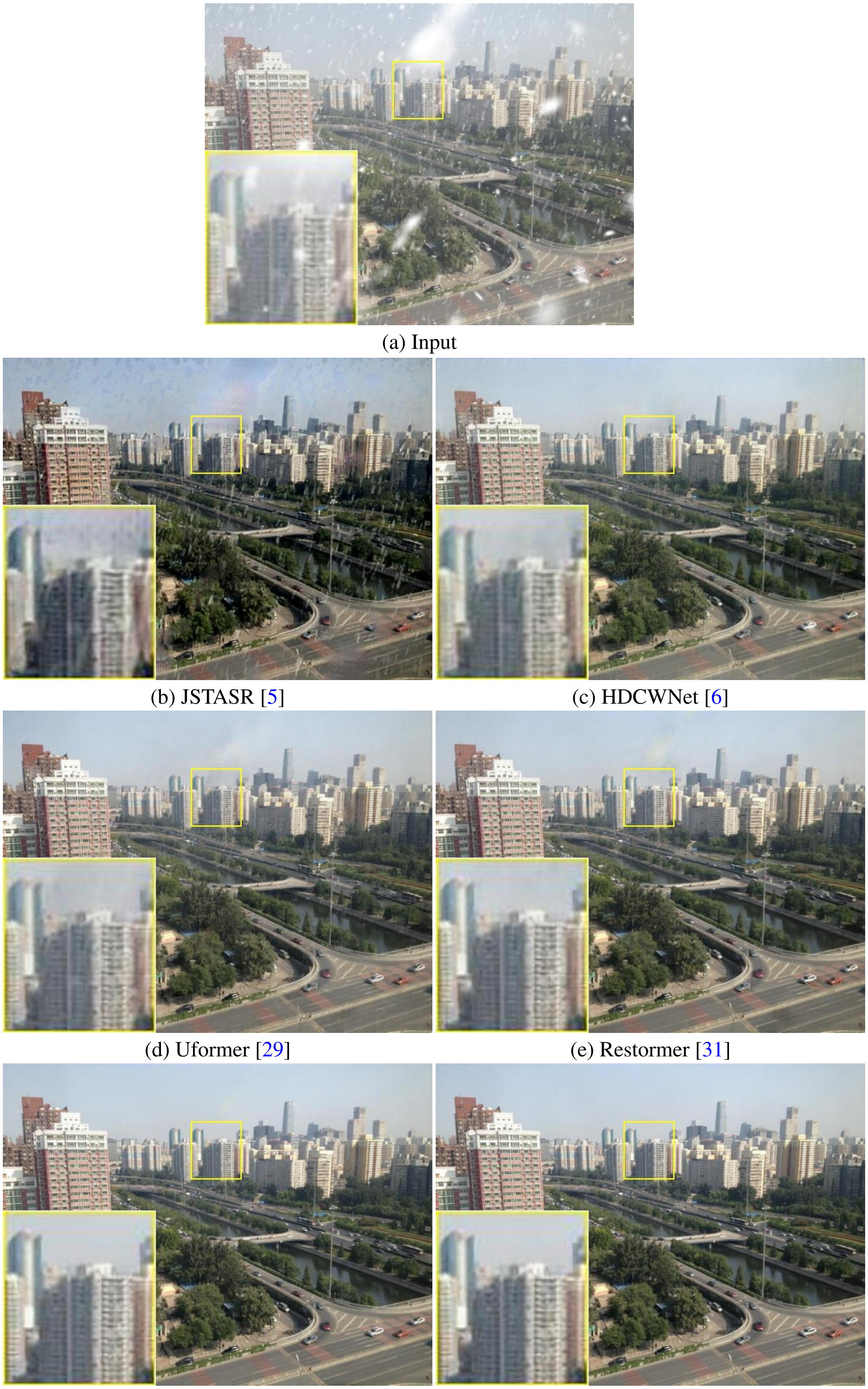

(a) Input

(b) JSTASR [5]

(c) HDCWNet [6]

(d) Uformer [29]

(e) Restormer [31]

(f) PromptRestorer

(g) GT

Figure 38: **Image desnowing** example on CSD (2000) [6].

References

[1] C. O. Ancuti, C. Ancuti, M. Sbert, and R. Timofte. Dense-haze: A benchmark for image dehazing with dense-haze and haze-free images. In *ICIP*, pages 1014–1018, 2019.

[2] C. O. Ancuti, C. Ancuti, and R. Timofte. Nh-haze: An image dehazing benchmark with non-homogeneous hazy and haze-free images. In *CVPR workshops*, pages 444–445, 2020.

[3] C. Chen, X. Shi, Y. Qin, X. Li, X. Han, T. Yang, and S. Guo. Real-world blind super-resolution via feature matching with implicit high-resolution priors. In *ACM MM*, pages 1329–1338, 2022.

[4] S. Chen, T. Ye, Y. Liu, T. Liao, Y. Ye, and E. Chen. Msp-former: Multi-scale projection transformer for single image desnowing. *arXiv preprint arXiv:2207.05621*, 2022.

[5] W.-T. Chen, H.-Y. Fang, J.-J. Ding, C.-C. Tsai, and S.-Y. Kuo. Jstasr: Joint size and transparency-aware snow removal algorithm based on modified partial convolution and veiling effect removal. In *ECCV*, pages 754–770, 2020.

[6] W.-T. Chen, H.-Y. Fang, C.-L. Hsieh, C.-C. Tsai, I. Chen, J.-J. Ding, S.-Y. Kuo, et al. All snow removed: Single image desnowing algorithm using hierarchical dual-tree complex wavelet representation and contradict channel loss. In *ICCV*, pages 4196–4205, 2021.

[7] X. Chen, Z. Zhang, J. S. Ren, L. Tian, Y. Qiao, and C. Dong. A new journey from sdrtv to hdrtv. In *ICCV*, pages 4500–4509, 2021.

[8] Y. Cui, Y. Tao, Z. Bing, W. Ren, X. Gao, X. Cao, K. Huang, and A. Knoll. Selective frequency network for image restoration. In *ICLR*, 2023.

[9] H. Dong, J. Pan, L. Xiang, Z. Hu, X. Zhang, F. Wang, and M. Yang. Multi-scale boosted dehazing network with dense feature fusion. In *CVPR*, pages 2154–2164, 2020.

[10] X. Fu, J. Huang, D. Zeng, Y. Huang, X. Ding, and J. Paisley. Removing rain from single images via a deep detail network. In *CVPR*, 2017.

[11] J. Gu, H. Lu, W. Zuo, and C. Dong. Blind super-resolution with iterative kernel correction. In *CVPR*, 2019.

[12] C.-L. Guo, Q. Yan, S. Anwar, R. Cong, W. Ren, and C. Li. Image dehazing transformer with transmission-aware 3d position embedding. In *CVPR*, pages 5812–5820, 2022.

[13] J. He, Y. Liu, Y. Qiao, and C. Dong. Conditional sequential modulation for efficient global image retouching. In *ECCV*, volume 12358, pages 679–695. Springer, 2020.

[14] K. He, X. Zhang, S. Ren, and J. Sun. Deep residual learning for image recognition. In *CVPR*, pages 770–778, 2016.

[15] K. Jiang, Z. Wang, P. Yi, B. Huang, Y. Luo, J. Ma, and J. Jiang. Multi-scale progressive fusion network for single image deraining. In *CVPR*, 2020.

[16] B. Li, W. Ren, D. Fu, D. Tao, D. Feng, W. Zeng, and Z. Wang. Benchmarking single-image dehazing and beyond. *TIP*, 28(1):492–505, 2019.

[17] X. Li, J. Wu, Z. Lin, H. Liu, and H. Zha. Recurrent squeeze-and-excitation context aggregation net for single image deraining. In *ECCV*, 2018.

[18] Y. Li, R. T. Tan, X. Guo, J. Lu, and M. S. Brown. Rain streak removal using layer priors. In *CVPR*, 2016.

[19] X. Liu, Y. Ma, Z. Shi, and J. Chen. Griddehazenet: Attention-based multi-scale network for image dehazing. In *ICCV*, pages 7313–7322, 2019.

[20] Y.-F. Liu, D.-W. Jaw, S.-C. Huang, and J.-N. Hwang. Desnownet: Context-aware deep network for snow removal. *TIP*, 27(6):3064–3073, 2018.

[21] Z. Liu, H. Mao, C.-Y. Wu, C. Feichtenhofer, T. Darrell, and S. Xie. A convnet for the 2020s. In *CVPR*, pages 11976–11986, 2022.

[22] S. Nah, T. Hyun Kim, and K. Mu Lee. Deep multi-scale convolutional neural network for dynamic scene deblurring. In *CVPR*, 2017.

[23] J. Rim, H. Lee, J. Won, and S. Cho. Real-world blur dataset for learning and benchmarking deblurring algorithms. In *ECCV*, 2020.

[24] Z. Shen, W. Wang, X. Lu, J. Shen, H. Ling, T. Xu, and L. Shao. Human-aware motion deblurring. In *ICCV*, 2019.

[25] X. Tao, H. Gao, X. Shen, J. Wang, and J. Jia. Scale-recurrent network for deep image deblurring. In *CVPR*, 2018.

[26] C. Wang, X. Xing, Y. Wu, Z. Su, and J. Chen. DCSFN: deep cross-scale fusion network for single image rain removal. In *ACM MM*, pages 1643–1651, 2020.

[27] X. Wang, K. Yu, C. Dong, and C. C. Loy. Recovering realistic texture in image super-resolution by deep spatial feature transform. In *CVPR*, 2018.

[28] X. Wang, K. Yu, C. Dong, and C. C. Loy. Recovering realistic texture in image super-resolution by deep spatial feature transform. In *CVPR*, 2018.

[29] Z. Wang, X. Cun, J. Bao, and J. Liu. Uformer: A general u-shaped transformer for image restoration. *arXiv:2106.03106*, 2021.

[30] W. Yang, R. T. Tan, J. Feng, J. Liu, Z. Guo, and S. Yan. Deep joint rain detection and removal from a single image. In *CVPR*, pages 1685–1694, 2017.

[31] S. W. Zamir, A. Arora, S. Khan, M. Hayat, F. S. Khan, and M.-H. Yang. Restormer: Efficient transformer for high-resolution image restoration. In *CVPR*, pages 5718–5729, 2022.

[32] S. W. Zamir, A. Arora, S. Khan, M. Hayat, F. S. Khan, M.-H. Yang, and L. Shao. Multi-stage progressive image restoration. In *CVPR*, 2021.

[33] H. Zhang and V. M. Patel. Density-aware single image de-raining using a multi-stream dense network. In *CVPR*, 2018.

[34] H. Zhang, V. Sindagi, and V. M. Patel. Image de-raining using a conditional generative adversarial network. *IEEE TCSVT*, 30(11):3943–3956, 2020.

[35] Z. Zheng, W. Ren, X. Cao, X. Hu, T. Wang, F. Song, and X. Jia. Ultra-high-definition image dehazing via multi-guided bilateral learning. In *CVPR*, pages 16185–16194, 2021.